REPORT DOCUMENTATION PAGE

Form Approved
OMB No. 0704-0188

1. AGENCY USE ONLY (Leave blank)	2. REPORT DATE	3. REPORT TYPE AND DATES COVERED
	Dec 94	

4. TITLE AND SUBTITLE
Hybrid Fuzzy logic Control to stabilize an Inverted Pendulum From Arbitrary Initial Conditions

5. FUNDING NUMBERS

6. AUTHOR(S)
Michael J. deSilva

7. PERFORMING ORGANIZATION NAME(S) AND ADDRESS(ES)
AFIT Students Attending:
Univ of Washington

8. PERFORMING ORGANIZATION REPORT NUMBER
AFIT/CI/CIA
94-174

9. SPONSORING / MONITORING AGENCY NAME(S) AND ADDRESS(ES)
DEPARTNEMT OF THE AIR FORCE
AFIT/CI
2950 P STREET, BDLG 125
WRIGHT-PATTERSON AFB OH 45433-7765

10. SPONSORING / MONITORING AGENCY REPORT NUMBER

11. SUPPLEMENTARY NOTES

12a. DISTRIBUTION / AVAILABILITY STATEMENT
Approved for Public Release IAW AFR 190-1
Distribution Unlimited
BRIAN D. GAUTHIER, MSgt, USAF
Chief Administration

12b. DISTRIBUTION CODE

13. ABSTRACT *(Maximum 200 words)*

14. SUBJECT TERMS

15. NUMBER OF PAGES
76

16. PRICE CODE

17. SECURITY CLASSIFICATION OF REPORT	18. SECURITY CLASSIFICATION OF THIS PAGE	19. SECURITY CLASSIFICATION OF ABSTRACT	20. LIMITATION OF ABSTRACT

HYBRID FUZZY LOGIC CONTROL TO STABILIZE AN INVERTED PENDULUM FROM ARBITRARY INITIAL CONDITIONS

by

Michael J deSylva

A thesis submitted in partial fulfillment
of the requirements for the degree of

Master of Science in Aeronautics and Astronautics

University of Washington

1994

Approved by _____
(Chairperson of Supervisory Committee)

Program Authorized
to Offer Degree Department of Aeronautics and Astronautics

Date December 13, 1994

Table of Contents

List of Figures

List of Tables

Chapter 1

Introduction

1.1 Motivation

Fuzzy logic is gaining increasing interest in the controls community. It is one of several control schemes, including neural network and genetic algorithm based controllers, which are considered unconventional. Fuzzy logic is currently a subject of heated debate. Proponents claim that a good fuzzy logic controller can be designed without precise knowledge of the plant. The designer can build up the controller based on a general idea of what it must accomplish. It is for this reason that fuzzy logic is particularly useful in instances where a human operator is being replaced, or where a human has an implicit model in mind of the input-output behavior of a system. For example, in Japan, the Sendai subway is now controlled by fuzzy logic. Replacing the human driver, it pulls into the station within a few inches of its target[1]. Successes such as this are used to re-enforce the claims for the power of fuzzy logic control.

Traditional techniques such as proportional-integral-derivative (PID) control or linear quadratic regulators (LQR) make use of a set of gains, which must be calculated based on precise system dynamics described by the mathematical model. This often presents a problem when dealing with systems that are of a very high order or that are highly nonlinear. In such cases it may be difficult to arrive at an accurate mathematical description of the system from which a controller can be synthesized. Fuzzy logic controllers circumvent these problems for the most part. Equations describing the system dynamics are formed only as a means of testing the controller before it is implemented on the hardware. Because the controller parameters are not based on these equations, modeling inaccuracies do not result in a poor controller.

Another reason for the recent interest in fuzzy logic controllers is their inherent robustness property. Because of the "fuzzy" nature of the controller, variations in system parameters are handled with ease. However, all evidence of robustness is ei-

ther from simulations or experiments as no mathematical proofs of robustness can be constructed. In a well-written paper, Abramovitch[1] points out that fuzzy logic is not a magical control technique that can solve every problem and provides a balanced view of the pros and cons of fuzzy logic control. For example, because fuzzy logic controllers rely on sample rates that are high relative to the system dynamics as well as a "common sense" control situation, there are clearly some situations where fuzzy logic will not work well. For fast systems with a complex input-output relationship, other control schemes may be more appropriate.

The inverted pendulum is one of the most popular workspaces on which to test non-linear control schemes. For the research presented in this thesis, the single link Linear Track Cart-Pendulum (LTCP-1) in the University of Washington Control Systems Laboratory (UWCSL) is used. It has a fairly conventional mechanization where the pendulum is hinged to a cart which moves back and forth along a linear track. This pendulum setup is an ideal test bed for the fuzzy logic controller for several reasons. The cart movement required to balance the pendulum is very intuitive. If a human could react quickly enough, it would be easy to balance it manually. The fuzzy controller can essentially speed up the human reactions. In addition, it is inherently unstable about the equilibrium point, making feedback control a necessity. The inverted pendulum is also a single input, multi output (SIMO) system that exhibits non-negligible nonlinearities due to friction forces, backlash, and dead zones. These nonlinearities are especially significant at large angle excursions. Because a linear model is unnecessary to design a fuzzy logic controller, these problems are not as significant as with other control schemes.

1.2 Problem Definition

The primary objective is to develop a fuzzy logic controller that will balance the inverted pendulum starting from any initial conditions for the pendulum while keeping the cart within the track bounds. The pendulum may start off in a balanced position already, it may start off hanging or it may start off with some random angle

and angular rate. Regardless of the set of initial conditions, the controller should move the cart back and forth within the bounds of the track so that the pendulum swings up to the balanced position and stays there. It is in the *swinging* or *pump up* phase of control that the nonlinearities and discontinuities become especially important.

1.3 System Description

The linear cart-pendulum in the UWCSL has the basic layout shown in figure 1.1. There is one optical encoder on the right pulley to sense linear track position (z), and a second one at the base of the pendulum to sense the angle (θ). The cart is moved back and forth along the track by the belt-pulley system, which consists of two pulleys and a slotted timing belt. The timing belt goes around both pulleys and through the cart. The left pulley is connected to a DC motor which provides the necessary torque. The belt and pulley convert this torque to a force on the cart which provides the desired acceleration. The pendulum is swung back and forth and then held in the upright position by moving the cart as necessary. A sampling time of 10 milliseconds was used. For a more detailed description of the hardware configuration, see Appendix B.

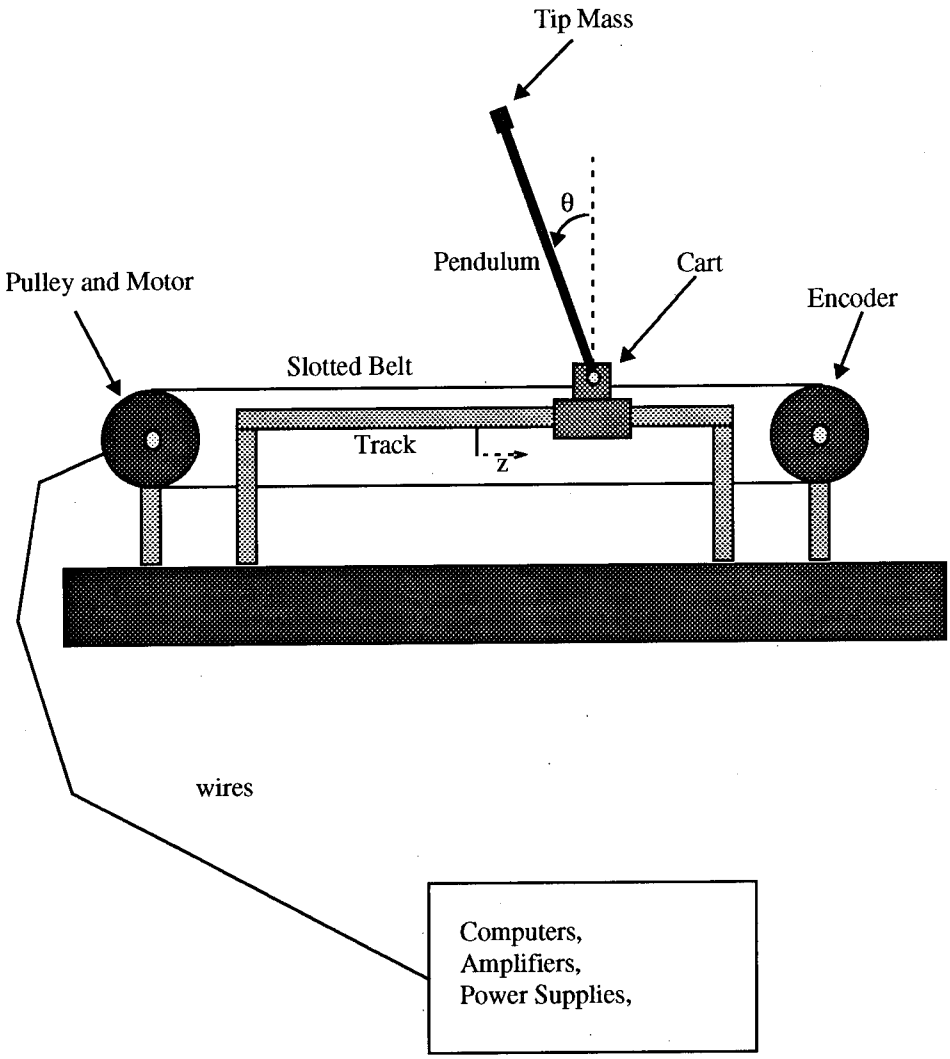

Figure 1-1 LCTP-1 in UWCSL

1.4 Software Description

Modeling, controller design, and simulation were all accomplished using SystemBuild software by Integrated Systems Inc. (ISI) in Santa Clara, California[13]. This software is run on a Sun Electronics SPARCstation10. The SystemBuild environment is block diagram oriented. Both the nonlinear system model and the controller were formed using blocks in the SystemBuild Block Library. There is a

fuzzy logic block that can be connected with the other SystemBuild blocks, making for easy integration of the fuzzy controller with the nonlinear model and the other controller parameters. The fuzzy logic block is different than the other blocks however. It is actually a tool box, rather than a simple one function building block. Within the fuzzy logic tool box, membership functions and rule bases may be defined, fuzzification and defuzzification methods may be selected, and optimization preferences may be chosen. It does have limitations however, which are outlined in section 5.2.

The AC100 software, also developed by ISI, was used to generate the C code, then compile it and link it for hardware implementation. The compiling, linking, and real time running are performed on a Dell 466/m computer equipped with the necessary input/output hardware. The C code itself is transferred via ethernet to the Dell. The AC100 software is very flexible and allows for the inclusion of a graphical user interface (GUI). The GUI, also referred to as an Interactive Animation Window allows the user to change system parameters with the controller "on line", monitor sensor and controller output information, and record data as desired. It runs on the SPARCstation, but communicates with the controller through the ethernet.

1.5 Previous Work

Many other researchers have applied fuzzy logic control theory to solve the stabilization problem for the inverted pendulum[10][11][14][23][28]. Ostertag and Carvalho-Ostertag [23]developed a fuzzy controller for a similar cart and track inverted pendulum. They compared the performance achieved using the fuzzy controller to that using a full state feedback controller. The results were encouraging in that the fuzzy controller performed at least as well as the model-based state feedback controller. They also tested a fuzzy friction compensator, very similar to the one developed in this research. When implemented with the fuzzy logic controller, it worked at least as well as the disturbance observer implemented with the full state feedback controller.

Katai and Ida[14] developed a fuzzy logic controller for the inverted pendulum

that worked based on goal decoupling. They constructed a controller such that the total goal of control was decomposed into a goal for the pendulum subsystem and a goal for the cart subsystem. They did this using *constraint oriented fuzzy inference.* Essentially, they put constraints on the fuzzy rules such that the cart does not hit the edge of the track and the pendulum does not fall down. They achieved good results using this innovative and simple technique.

These and other researchers have managed to control the pendulum when it starts off in the balanced position, but nobody has investigated the ability of a fuzzy logic controller to stabilize the pendulum vertically from any arbitrary set of initial conditions. Some research has been done using other techniques, however. Wiklund, Kristenson, and Astrom[18] did some work on an inverted pendulum that is configured a little bit differently than the LCTP-1. It was modeled after the Toykyo Institute of Technology Pendulum shown in Figure 1-2.

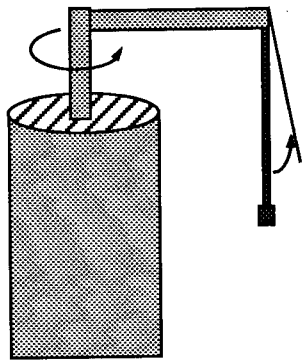

Figure 1-2 TIT Pendulum

They successfully developed an energy based controller to swing up the pendulum based on any initial conditions. They used feedback linearization for the balancing phase and a differential equation including energy for the pump up control law. Their pump up control law does not use full motor torque unless the total energy is zero which slows the energy augmentation. This pendulum configuration allows the motor to more directly affect the pendulum resulting for quicker actuation. It also eliminates the rail constraint. These aspects serve to simplify the control problem.

Chapter 2

Fuzzy Logic Control Theory

Fuzzy logic is a tool for relating qualitative information and combining it in a way that produces useful results. This qualitative information is called fuzzy data and decisions are made based on a set of rules that relates this data to a desired response. This set of rules is called the knowledge base which is usually in an if-then format with a condition and an assertion. One example of such a rule can come directly from the pendulum system. If the pendulum is *slightly* off balance to the right and falling *rapidly* to the right, then the cart should move *rapidly* to the right in an attempt to catch it. Slightly and rapidly are vague descriptions of system data rather than the concrete numerical values that are output from the encoders. This is what is meant by fuzzy data. The concrete values are called crisp data, which is what is input into the controller in most circumstances. As a result, the controller must go through a three step process in order to arrive at the desired output signals based on the input signals. One is fuzzification, two is rule base evaluation, and three is defuzzification. Dubois and Prade[6] provide an excellent foundation in fuzzy logic theory if the following discussion is not detailed enough.

2.1 Fuzzification

Fuzzification involves converting the crisp input data into qualitative information that can be related by the fuzzy rules. This is done by assigning a belief value to each crisp input based on class or concept. These belief values fall on a scale from zero to one, with zero meaning definitely false and one meaning definitely true. It is helpful to use a simple example to clarify this concept.

Consider a prospective home buyer who is worried about his payments. If the house is expensive and the interest rate is high, then the monthly payments will be high. The price of the house, and the interest rate are both specific values which must be fuzzified before this relation can be made. If 100% of the people in his income

bracket consider a house costing $200,000 to be expensive and 0% consider one costing $100,00 expensive, then what might be said of a house costing $150,000? The home buyer might say that it is somewhat expensive. There is a whole range between not expensive and expensive that cannot be strictly classified as either of the two. To fuzzify the data, a membership curve must be designed so that at $100,000 the belief that the house is expensive is zero, at $200,000 it is one, and between the two prices it has some intermediate value. Based on the triangular membership function shown in Figure 2-1, the $150,000 house would be considered expensive to a degree of 0.5. An interest rate of 9.0 would be considered high to a degree of 0.5 as well.

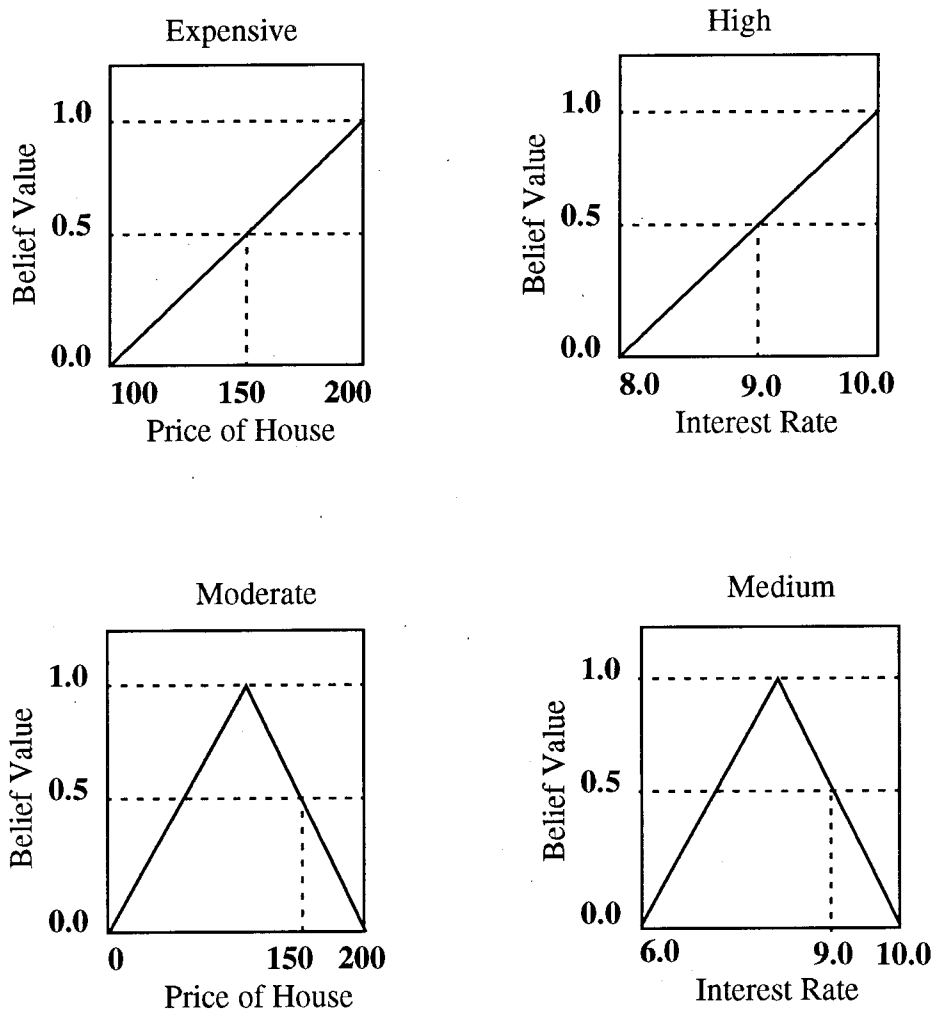

Figure 2-1 Membership Curve Examples

In most cases, there will be more than one membership function which the data intersects. For example, in Figure 2-1, curves have also been defined for what is considered a moderately priced home as well as a medium interest rate. The curves overlap some of the region covered by the expensive and high curves. By considering them as well, the price of $150,000 is considered expensive to a degree of 0.5 and moderate to a degree of 0.5. Similarly, an interest rate of 9.0 is considered high to a degree of 0.5 and medium to a degree of 0.5. Any rule containing an expensive or moderate house and a high or medium interest rate will be activated to some extent by that fuzzy data.

Membership curves need not be composed of simple linear triangles such as have been used in the illustration here. Sine and cosine functions are commonly used. Often a population of sampled data is used to form the membership functions so that they make statistical sense. In general, they may be formed as necessary to arrive at the desired fuzzy interpretation of the crisp data. Regardless of the shape, the fuzzification is accomplished by checking the belief value at which the crisp datum intersects the membership curve.

2.2 Rule Base Evaluation

Rule Base Evaluation, often termed Implication refers to the application of the knowledge base to the fuzzy data. It results in a set of fuzzy output or control variables.

2.2.1 Knowledge Base

The knowledge base forms the core of the fuzzy logic controller and is where most of the design flexibility resides. Used in this context, *knowledge* refers to the qualitative control information which has been organized in the form of a set of rules. These rules take the form of simple *if-then* statements. A good illustration is a typical braking situation in an automobile. If a person is driving fast, and he must stop in a short distance, then he must apply the brakes hard. Intuitively this makes sense, but it is difficult to apply this information using mathematical equations. This is especially true if the mechanics of braking are not well understood. The qualitative nature

of fuzzy logic allows for the easy implementation of this type of intuitive knowledge. The size of the knowledge base is dependent on the number of membership curves and subdivisions in each curve. In the braking example, if there are three subdivisions in the membership curve for driving speed and three subdivisions in the membership curve for stopping distance, then the rule base will be three by three.

2.2.2 Implication

Implication refers to forming the fuzzy control variable based on the data and the rules. For all of the fuzzy controllers in this paper the Mamdani method is used. It makes use of the minimum operator to come up with a belief value in the output of a rule. An example is again useful for illustration. Referring back to the mortgage payment example, the rule was "if the house is expensive and the interest rate is high, then the payments are high." The belief that the payment is high is related to the minimum of the belief that the house is expensive and the belief that the interest rate is high.

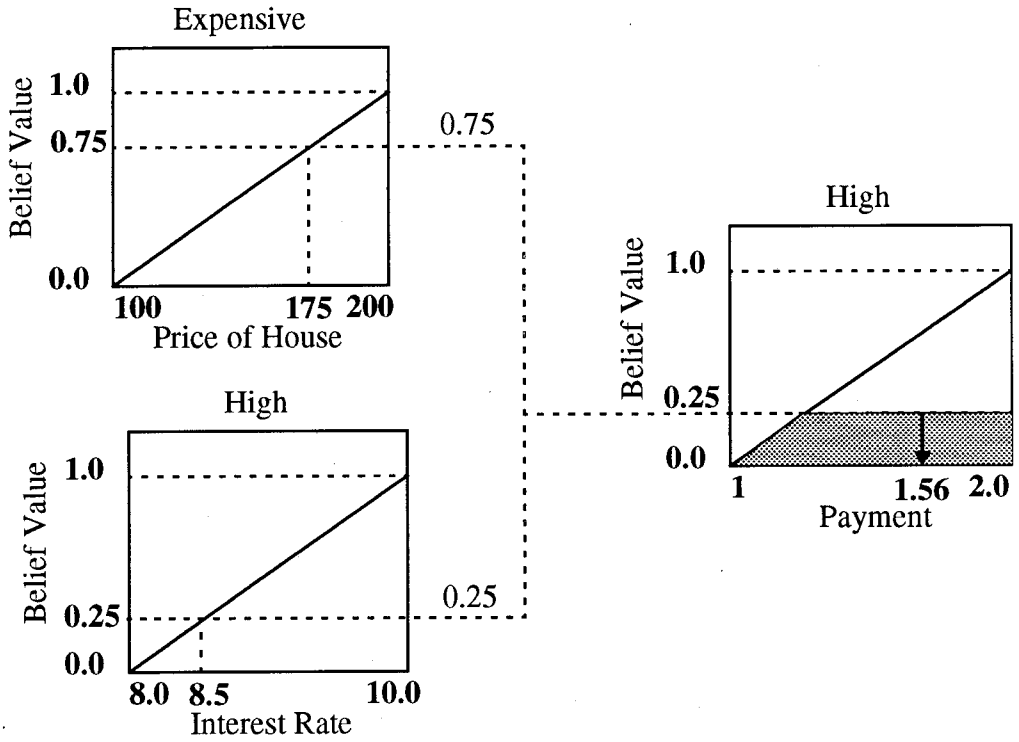

Figure 2-2 Mamdani Implication

Therefore, if the house is expensive to a degree of 0.75 and the interest rate is high to a degree of 0.25, then the payments curve will be leveled off at a belief value of 0.25. This leveled off curve describes the fuzzy payment variable.

2.3 Defuzzification

Defuzzification is the converting of the fuzzy control variable to a crisp output that can be used as a control. This step is very similar to fuzzification except that the leveled off curve provides for many possible payment values when the belief that the payment is high is 0.25. The actual payment might be anywhere from 1.25 to 2.0. For the defuzzification used in this research, the centroid method was used to deduce the crisp payment value. Essentially, the leveled off curve is split up so that there are equal areas on each side of a division. The division point is then the real-valued output. For the example above, the payment would be 1.56 determined as follows

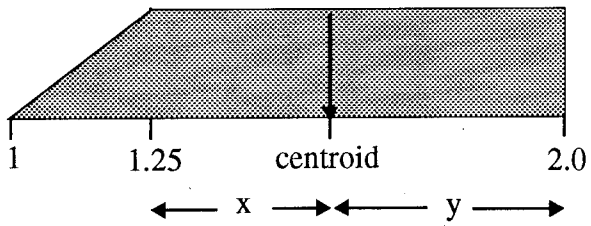

Figure 2-3 Centroid Calculation Diagram

by equating areas on either side of the centroid

$$\frac{0.25^2}{2} + 0.25x = 0.25y \qquad (2\text{-}1)$$

which can be simplified to yield

$$x - y = -\frac{0.25}{2} \qquad (2\text{-}2)$$

because the total distance must add up to one

$$x + y = 0.75 \qquad (2\text{-}3)$$

adding *(2-2)* to *(2-3)* the centroid can be determined

$$x = 0.31 \Rightarrow centroid = 0.56 \qquad (2\text{-}4)$$

In most cases, more than one rule will be activated by the fuzzy input variables. When this occurs, the rules must be processed in parallel and a weighted average taken. This process is referred to as aggregation. An arithmetic mean with each rule having an equal weight was used for the research presented here.

Chapter 3

Controller Design

3.1 Introduction/Design Process

The eventual goal of balancing the pendulum and centering the cart from any set of consistent initial conditions may be broken down into several independent subtasks. Among these are balancing the pendulum, centering the cart, and swinging up the pendulum. To simplify the design process and better isolate problems, each of these tasks was performed separately. First, the fuzzy controller for stabilizing the pendulum about its unstable equilibrium point was developed and tested in simulation. Then an outer loop containing another fuzzy controller was added to center the cart. This was then tested and adjusted in both simulation and hardware. Finally, an energy based fuzzy logic controller was added to the inner loop in order to swing the pendulum up to the balanced range from extreme initial conditions. The combination of information about the state space and energy leads to the term "hybrid fuzzy logic" control. To use energy, we must have some type of model available to the system. The integration of the three fuzzy controllers was performed at each step.

These tasks had to be accomplished while respecting the physical constraints imposed by the hardware. The most important of these are the limited motor voltage and the limited rail length. Both prove to be very significant in the pump up phase of control. In order to reduce the effects of friction on the controller's performance, a fuzzy friction compensator has also been developed. This helps overcome both dry and viscous friction forces. The friction coefficient between the cart and the rail on the LCTP-1 is constantly changing. As a result, the fuzzy compensator is better suited to overcoming the friction than other techniques such as constant threshold switching. The full controller block diagram is shown and explained in Section 3.6 on system integration.

3.2 Balancing

This task was accomplished first, without taking into account the position of the cart on the rail. The two inputs to this controller are the angular error (θ_e deg) and the angular rate (θ_d deg/sec). The angular error is simply the current angle (θ) subtracted from the reference angle ($\theta_{ref} = 0$ for this phase of the design). The angular rate is calculated based on the angular variation in one sampling period. The output of this controller is the control voltage (E_c) which is sent to the plant through a D/A converter and an amplifier. The rule base was formulated based on an intuitive notion of how the cart must move in order to balance the pendulum. For example, if the pendulum is inclined and falling to the right, then it makes sense that the cart should accelerate to the right to catch the pendulum. Once the rule base was formed, very few adjustments were made. The membership curves provide more flexibility for the tuning of the controller. Simple triangular and quadrilateral shapes were used to form the classes. The width and center for each member's curve were initially determined based on kinetic energy calculations. Adjustments were then made as necessary, based on the simulation results.

SystemBuild has a couple of useful intrinsic functions which were utilized to formulate the membership curves. The function QUAD defines a quadrilateral with the four corners specified laterally by the points indicated. The first and last points are automatically defined as zero and the second and third points one on the longitudinal axis. Similarly, TRG defines a triangle with the three corners as specified, and the second point representing a belief value of one. The membership equations for θ_e are shown in Table 3.1. Figure 3-2 shows a graphical interpretation of the curves. The real-valued input was broken down into five fuzzy classes, Negative Big, Negative Small, Zero, Positive Small, and Positive Big.

Table 3-1 θ_e Membership Curve Equations for Bal

NB	QUAD (X,-10,-10,-2,-1)
NS	TRG (X,-2,-1,0)
Z	TRG (X,-1,0,1)
PS	TRG (X,0,1,2)
PB	QUAD (X,1,2,10,10)

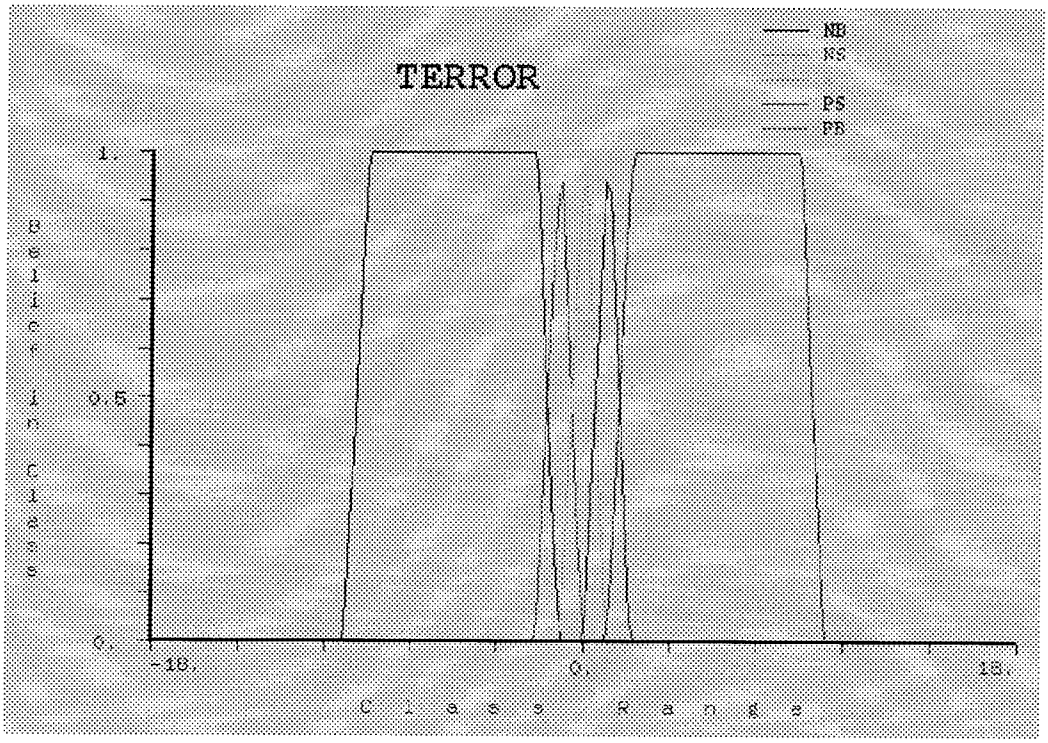

Figure 3-1 θ_e Membership Curves

The membership equations for the second input, θ_d, are shown in Table 3-2. Again, the crisp input was broken down into five fuzzy classes, Negative Big, Negative Small, Zero, Positive Small, and Positive Big. The plots for this and all of the membership curves hereafter are shown in Appendix E.

Table 3-2 θ_d Membership Curve Equations for Bal

NB	QUAD (X,-19,-19,-10,-5)
NS	TRG (X,-10,-5,0)
Z	TRG (X,-5,0,5)
PS	TRG (X,0,5,10)
PB	QUAD (X,5,10,19,19)

Finally the membership equations for the defuzzification of the output, E_c, are shown in Table 3-3. The number of divisions for the output may be increased without adding dimension to the rule base. For the control voltage, Negative Medium and Positive Medium were included in addition to the five standard classes. This is an "inexpensive" way to add resolution to the controller without significantly increasing computation time.

Table 3-3 E_c Membership Curve Equations for Bal

NB	QUAD (X,-10,-9,-8,-4)
NM	TRG (X,-8,-4,-2)
NS	TRG(X,-4,-2,0)
Z	TRG(X,-2,0,2)
PS	TRG (X,0,2,4)
PM	TRG (X,2,4,8)
PB	QUAD (X,4,8,9,10)

Now that the membership curves have been defined for the two inputs and the one output, the rule base may be formulated. As indicated earlier, this is where the intuitive nature of fuzzy logic becomes useful and apparent. Because the variables are fuzzy, conceptual ideas of what must happen in order to keep the pendulum vertical are more important than the exact mathematical model. Table 3-4 shows the rule

base that results from these conceptual ideas.

Table 3-4Balancing Rule Base

θ_d \ θ_e	NB	NS	Z	PS	PB
NB	Z	PS	PM	PB	PB
NS	NS	Z	PS	PM	PB
Z	NM	NS	Z	PS	PM
PS	NB	NM	NS	Z	PS
PB	NB	NB	NM	NS	Z

The body of the table is the control voltage. For example, the first rule is "if θ_e is NB and θ_d is NB, then E_c is Z." Essentially, this states that if the pendulum is tilted significantly to the right, and it is swinging quickly up to the left, then the cart need not accelerate in either direction. Given this set of conditions, the pendulum should swing itself up to the balanced position without any external control.

3.3 Centering

Once the balancing controller is working in simulation, a centering loop must be added so that the cart does not wander to the edges of its operating range. This was done by adding an outer loop to the balancing task as shown in Figure 3-2.

The inputs to the balancing controller are a reference angle and the actual pendulum angle with respect to the vertical. Changing the reference angle forces the cart to move in one direction or the other. Therefore, the controller can generate a reference angle that will drive the cart towards the center.

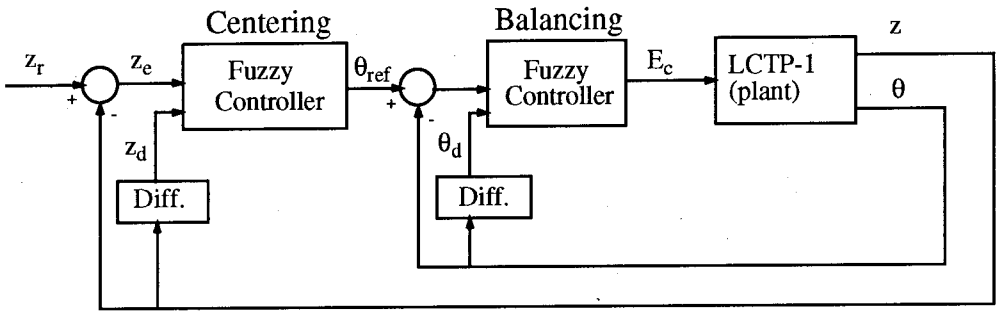

Figure 3-2 Balancing and Centering Controller

The inputs to this centering controller are the position error (Z_e (m)) and the cart velocity (Z_d (m/s)). The position error is simply the actual position (Z (m)) subtracted from the reference position (Z_{ref} (m)). The output is θ_{ref}. Again, the membership curves for the three data must be defined before the conceptual rule base can be implemented. The equations are below and the plots are shown in Section E.2.

Table 3-5 Z_e Membership Curve Equations for Ctr

NB	QUAD (X,-3,-3,-0.1,-0.02)
NS	TRG (X,-0.1,-0.02,0)
Z	TRG (X,-0.02,0,0.02)
PS	TRG (X,0,0.02,0.1)
PB	QUAD (X,0.02,0.1,3,3)

In the design of the above membership curves for the position error, a deviation of 10 centimeters or more in either direction is considered large. An error of 2 centimeters is considered small. These effectively determine the range of the limit cycle on position and are chosen based on what is acceptable and reasonable.

Table 3-6 Z_d Membership Curve Equations for Ctr

NB	QUAD (X,-3,-3,-0.5,-0.2)
NS	TRG (X,-0.5,-0.2,0)
Z	TRG (X,-0.2,0,0.2)
PS	TRG (X,0,0.2,0.5)
PB	QUAD (X,0.2,0.5,3,3)

The membership class ranges for the cart velocity were based on results from the balancing simulations. The cart velocity is run through a low pass filter with a cutoff frequency of 10 rad/sec. This is designed to eliminate the spikes and yield general velocity trends which are more important for the cart centering.

Table 3-7 θ_{ref} Membership Curve Equations for Ctr

NB	QUAD (X,-2,-1,-0.5,-0.25)
NS	TRG (X,-0.5,-0.25,0)
Z	TRG (X,-0.25,0,0.25)
PS	TRG (X,0,0.25,0.5)
PB	QUAD (X,0.25,0.5,1,2)

The reference angles for the θ_{ref} membership curves were initially based on results from the balancing simulation, but then modified based on the experimental results. The final values are shown in Table 3-7.

In an ideal situation the cart is centered and the reference angle is zero so that the pendulum remains balanced perfectly upright. If the cart is offset in one direction however, the reference angle can be changed to force the cart back towards the center. For example, to hold the pendulum at an angle of 2 degrees to the right, the cart must move to the right with a constant acceleration to overcome the force of gravity. Therefore, if the cart is offset to the right, then the reference angle should be slightly

to the left forcing the cart to move back towards the center.

Table 3-8Centering Rule Base

Z_d \ Z_e	NB	NS	Z	PS	PB
NB	Z	Z	NS	NB	NB
NS	Z	Z	Z	NS	NB
Z	PS	PS	Z	NS	NS
PS	PB	PS	Z	Z	Z
PB	PB	PB	PS	Z	Z

3.4 Friction Compensation

Friction on the LCTP-1 is significant during all phases of control. This is primarily as a result of the bearings between the cart and the rail. There is an allen screw that tightens and loosens the contact between the cart, the bearings, and the rail. If it is over tightened, the motor is not strong enough to effectively overcome the friction and move the cart quickly enough. If it is too loose, then the cart is not secure on the rail leading to extra wear and a general sloppiness in the system. There is a point where the cart is secure and the friction is reasonable, but there is little margin either way.

There are two problems which must be dealt with by the controller. One is the dry and viscous friction which is present no matter how well tuned the allen screw is. If the controller outputs a certain voltage and the cart does not move, then the controller is ineffective during that sampling period. By the time it outputs a signal that can overcome the friction, the error is larger than it should have ever become and the controller has to overcompensate. The second problem is that the screw loosens with use, so that the coefficient of friction between the cart and the rail is constantly changing.

To deal with these problems a friction compensator of some sort must be added to the system. Because of the changing friction, a simple constant threshold switching compensator would not be entirely effective even at overcoming dry friction. Ostertag and Carvalho-Ostertag[23] did a comparison between several model based methods and a fuzzy compensator. They found that the fuzzy compensator was comparable and perhaps even better than the most sophisticated model based methods.

By using a fuzzy logic friction compensator based on the cart acceleration, we can overcome both dry and viscous friction simultaneously with a simple intuitive design. The inputs to the compensator are the control voltage from the main controller and the cart acceleration (Z_{dd} (m/s^2)). The control voltage is fuzzified into seven classes. It is important to know how much voltage is being applied so that an appropriately sized offset may be formulated. The acceleration is only fuzzified into three classes because it is sufficient to know whether it is accelerating and in which direction. The resulting rule base is thus seven by three. The output is an offset to be added to the control voltage before it is applied to the motor. It is fuzzified into five membership classes. All three sets of curves are defined below.

Table 3-9 E_c Membership Curve Equations for FC

NB	QUAD (X,-10,-10,-8,-6)
NM	TRG (X,-8,-6,-3)
NS	TRG(X,-6,-3,0)
Z	TRG(X,-3,0,3)
PS	TRG (X,0,3,6)
PM	TRG (X,3,6,8)
PB	QUAD (X,6,8,10,10)

Table 3-10 Z_{dd} Membership Curve Equations for FC

N	QUAD (X,-11,-11,-1,0)
Z	TRG (X,-1,0,1)
P	QUAD (X,0,1,11,11)

Table 3-11 $E_c$offset Membership Curve Equations for FC

NB	QUAD (X,-3,-3,-2,-1)
NS	TRG (X,-2,-1,0)
Z	TRG (X,-1,0,1)
PS	TRG (X,0,1,2)
PB	QUAD (X,1,2,3,3)

The rule base for the fuzzy friction compensator uses the same intuitive logic as the other fuzzy rule bases. For the LCTP-1, a constant voltage results in a constant force applied to the cart. If there were no friction, this would result in a constant acceleration. Therefore, if a voltage was applied during the previous sampling period and the cart is not accelerating in the appropriate direction, then the motion is being resisted by a static friction force. If an acceleration in the proper direction is observed but it is too small then a coulomb or viscous friction force is the culprit. The rule base is summarized in Table 3-12.

Table 3-12Friction Compensation Rule Base

Z_{dd} \ E_c	NB	NM	NS	Z	PS	PM	PB
N	NB	NS	Z	Z	Z	Z	Z
Z	NB	NB	NS	Z	PS	PB	PB
P	Z	Z	Z	Z	Z	PS	PB

When Z_{dd} is in the vicinity of zero the rules make sense for overcoming static friction. For example, if a negative big voltage is being applied and the cart still has zero acceleration, a large dry friction is resisting the motion and a negative big offset should be added to the control voltage. When the cart is actually accelerating in one direction or the other, then a viscous and/or coulomb friction is resisting the motion. The offset is added when the cart is accelerating in the proper direction. Since the fuzzy classes are not broken down into magnitudes of acceleration, the offset depends only on the control voltage. If the control voltage is negative big, then the offset is negative big. This is done to overcome the friction that is known to be present, and is very similar to constant threshold switching. To create a full rule base, zeros are filled in where the acceleration does not make sense relative to the voltage. For example a positive voltage cannot create a negative acceleration.

3.5 Pump Up

The swinging up of the pendulum is where the nonlinear aspects of the inverted pendulum become very apparent. The problem here is to bring the pendulum to the upright position from an arbitrary initial condition. This phase of control covers all four angular quadrants, resulting in significant discontinuities. The first controller attempted was a simple augmentation of the balancing controller. It was based on the angle and angular rate. It was ineffective because of several discontinuities. At ninety degrees from the vertical, the direction that the cart must move to swing the pendulum up or down changes. In addition, there is a decision point where the angle and angular rate are such that the controller should not attempt to immediately balance the pendulum, but rather let it swing up in the other direction. The voltages that should be applied on either side of these discontinuities is highly polar. Because these discontinuity points are not distinct in the fuzzy controller, it has a difficult time deciding which way to go. The negative big voltage being directed on one side of the discontinuity is cancelled by the positive big voltage which is necessary on the other side of the discontinuity. One possible option is to use another input, such as direc-

tional kinetic energy resulting in a three dimensional rule base. This however, is more computer intensive and harder to visualize.

Another approach is to consider total energy and design the controller such that it adds or subtracts energy. The goal would be a total energy equal to the potential energy when the pendulum is balanced. This is not an effective technique for balancing the pendulum however. If the pendulum is offset clockwise and moving clockwise, then energy would be added to the system by moving the cart left and letting the pendulum fall, rather than maintaining it vertically. The most effective way to deal with this problem is a deterministic rule. When the pendulum is within a certain range of the vertical, the balancing controller already developed will be used, otherwise the energy based pump up controller is invoked. This is further explained in Section 3.6.

The primary problem to be addressed by the energy based fuzzy controller is determining which direction the cart must move in order to adjust the energy. The second input to the controller is the one degree of freedom left from which this distinction can be made. A variable that indicates both the angular quadrant and the direction of rotation must be developed. This is illustrated by referring to Figure 3-3.

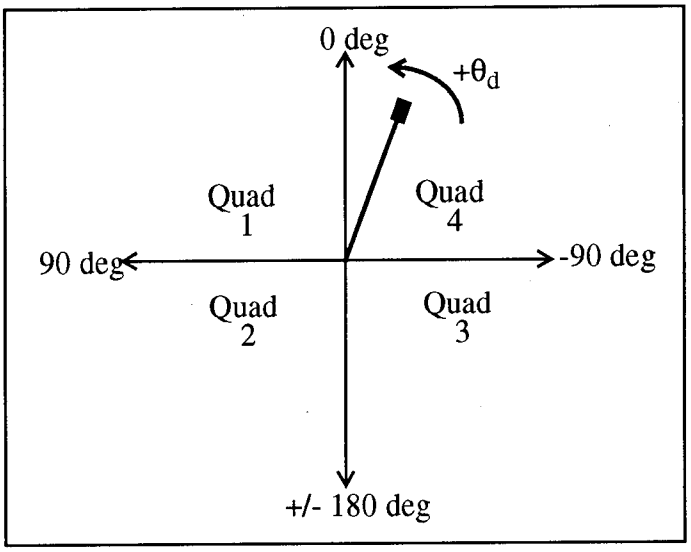

Figure 3-3 Pendulum Angular Quadrants

If the pendulum is in the first or fourth quadrants and the angular rate is positive, then energy can be added to the system by accelerating the cart to the right. Conversely, if the pendulum is swinging clockwise, then energy is added by accelerating to the left. Similarly, if the pendulum is in the second or third quadrant, and swinging positively, then energy can be added by accelerating the cart to the left. If the angular rate is negative, then energy is added by accelerating to the right. Energy can always be subtracted by moving in the opposite direction from that used to add energy. The task is to derive a variable that will tell both the quadrant and the direction of rotation. The function cosine is positive in quadrants one and two, which makes the necessary angular distinction. If cosine is then multiplied by the angular rate the quadrant and the direction are both distinguishable. A positive quantity indicates that the cart must accelerate to the right to add energy, and a negative number indicates that it must accelerate to the left to add energy.

Therefore, the two inputs to the pump up controller are total energy (TE), and the angular rate multiplied by the cosine of the angle ($\theta_d \cos\theta$). The total energy is calculated by adding the kinetic energy (T) to the potential energy (V).

$$TE = T + V \qquad (3\text{-}1)$$

The equations and system parameters used to calculate the energies are detailed in Appendix A. The cart energy is not used here and may be ignored. We are only interested in the pendulum.

The quantity $\theta_d \cos\theta$ is only being used to determine the proper direction to accelerate the cart, and has no impact on the exact size of the control voltage. The magnitude of this quantity is therefore unimportant. The large variations in magnitude that are possible actually present resolution problems for the controller. To avoid these problem, $\theta_d \cos\theta$ was normalized so that it was set equal to 5 for any positive value and -5 for any negative value. It is sufficient to fuzzify it into the three classes Negative, Zero and Positive which are defined in Table 3-13.

Table 3-13 $\theta_d \cos\theta$ Membership Curve Equations

N	TRG (X,-10,-5,0)
Z	TRG (X,-5,0,5)
P	TRG (X,0,5,10)

The magnitude of the system's total energy determines how much work the controller must do. The pump up phase is normally accomplished best using "bang bang" control. The knowledge that a minimum time pump up controller is bang bang comes from the application of Pontryagin's Maximum Principle to the nonlinear control problem[2]. This is full voltage applied in one direction or the other. As a result a simple three class fuzzification can be used to simplify the controller's computational requirements. When the controller is perfectly balanced, the kinetic energy is zero and the potential energy is equal to the total energy. This desired total energy is approximately 2.83 Joules.

$$PE = mgh = 0.324 \times 9.81 \times 0.890 = 2.83J \qquad (3\text{-}2)$$

To simplify the design of the membership curves, an offset is subtracted from the total energy so that the balanced state total energy is zero. It was also scaled up by a factor of five for better resolution. Refer to Section 5.2 for a discussion of why this scaling is necessary.

$$\text{TE into controller} = 5*(\text{Actual TE} - \text{Desired TE}) \qquad (3\text{-}3)$$

This allows the membership curves to be centered about zero. It also allows the desired total energy to directly influence the controller. It is sent in as an external input, so that the controller is easily adjustable to compensate for different pendulum lengths and tip masses. The classes are Big, Full, and Small. Big indicates that the there is too much energy currently in the system, and small indicates that there is currently too little. The equations describing the classes are outlined in Table 3-14.

Table 3-14 TE_{cont} Membership Curve Equations

N	QUAD (X,-11,-11,-1,0)
Z	TRG (X,-1,0,1)
P	QUAD (X,0,1,11,11)

Designing the rule base was again an intuitive task. When $\theta_d \cos\theta$ is zero, either the angular rate is zero or the pendulum is exactly horizontal. In either case, the controller should wait for the next sampling period before initiating any action. If the TE_{cont} is zero, then the pendulum has exactly the desired total energy and again, no action should be taken. If the TE_{cont} is Big, then energy should be subtracted from the system. Friction aids in removing energy, so that full voltage control inputs are unnecessary. If TE_{cont} is Small and energy must be added, full voltage inputs should be used to yield results similar to the optimum "bang bang" control. The resulting rule base is shown in Table 3.15.

Table 3-15Pump Up Rule Base

TE \ $\theta_d \cos(\theta_e)$	N	Z	P
N	PS	Z	NS
Z	Z	Z	Z
P	NB	Z	PB

3.6 Integration

The fuzzy controllers used for balancing, centering, pump up, and friction compensation are all separate entities which must be combined in a working fashion. The

SystemBuild block diagrams shown in Figures 3-4 and 3-5 detail the flow of the controller. The balancing and centering controllers tie together naturally, with the centering controller implemented as an outer loop wrapped around the balancing controller as shown in Figure 3-2. The friction compensation simply adds an offset to the control voltage. Therefore it is implemented immediately following the controller. It is block 3 in Figure 3-4.

The final task is to combine the pump up with the balancing and centering controller so that it works for the entire angular phase plane. Experimental testing has shown that the balancing controller can easily deal with an angular offset of +/- 10 degrees. In addition, once activated it will not allow excursions this large. The controller switching point was therefore chosen to be 10 degrees. See block 16 in Figure 3-5. Greater than that and the pump up controller is activated -- less than that and the balancing controller is used.

During the pump up phase, the cart position adjustment controller is ineffective, so that some precautionary measures have to be taken. When the pendulum is in the vicinity of 90 degrees, any cart movement will be relatively ineffective for energy adjustment. This provides an opportunity to make slight adjustments in the cart position. Another controller was developed that is used when the pendulum is within ten degrees either side of the horizontal. Block 15 in Figure 3-5 is the switching block for this controller. Based on the current cart position and velocity, the controller will use full voltage to move the cart towards the center. This adjustment simply allows for a little bit of extra maneuvering room. The cart will still slam into the edges of the rail. To prevent this, hard position limits were set on either side of center. These limits are external inputs into the controller and they come from the interactive animation window. The default limit is 0.4 meters. When the cart passes this limit, full voltage is applied towards the center of the rail. The rail length is 0.56, and this allows for deceleration if the cart is up to full speed when it hits the limits.

Discrete SuperBlock	Sampling Interval	First Sample	Ext.Inputs	Ext.Outputs	Enable
Fuzzy Controller	0.0100	0.	14	3	Parent

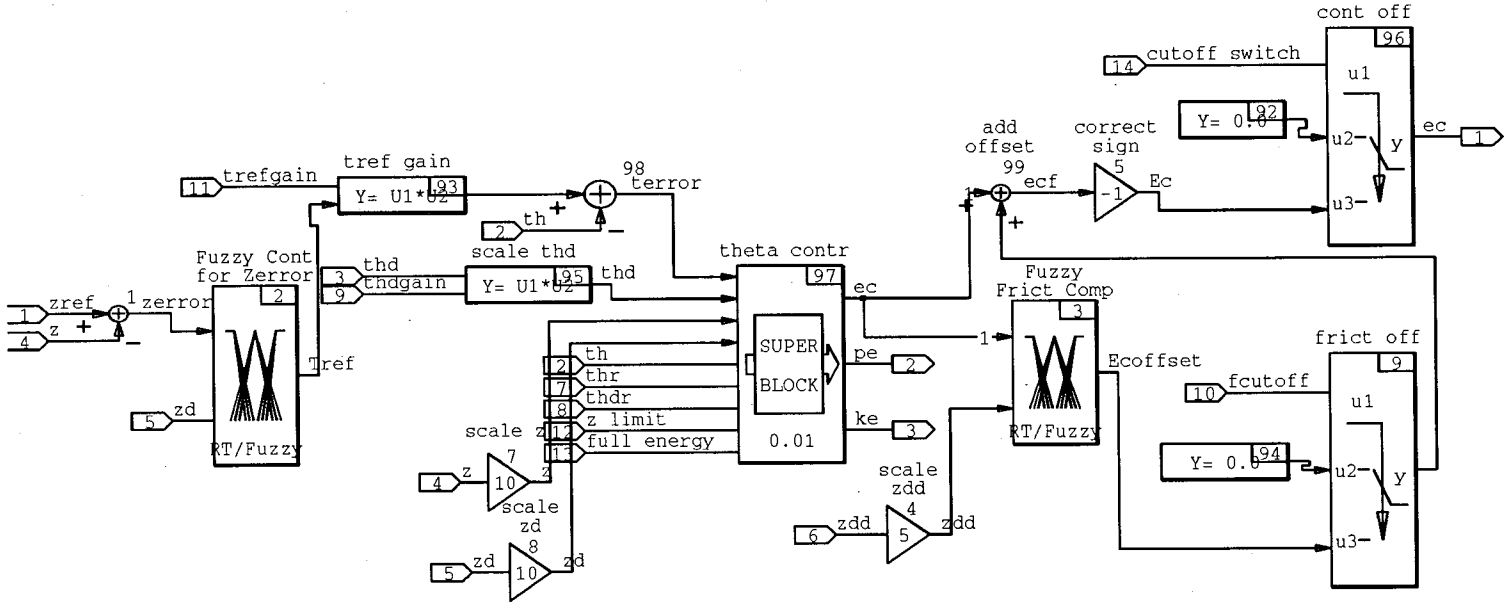

Figure 3-4 Full Controller

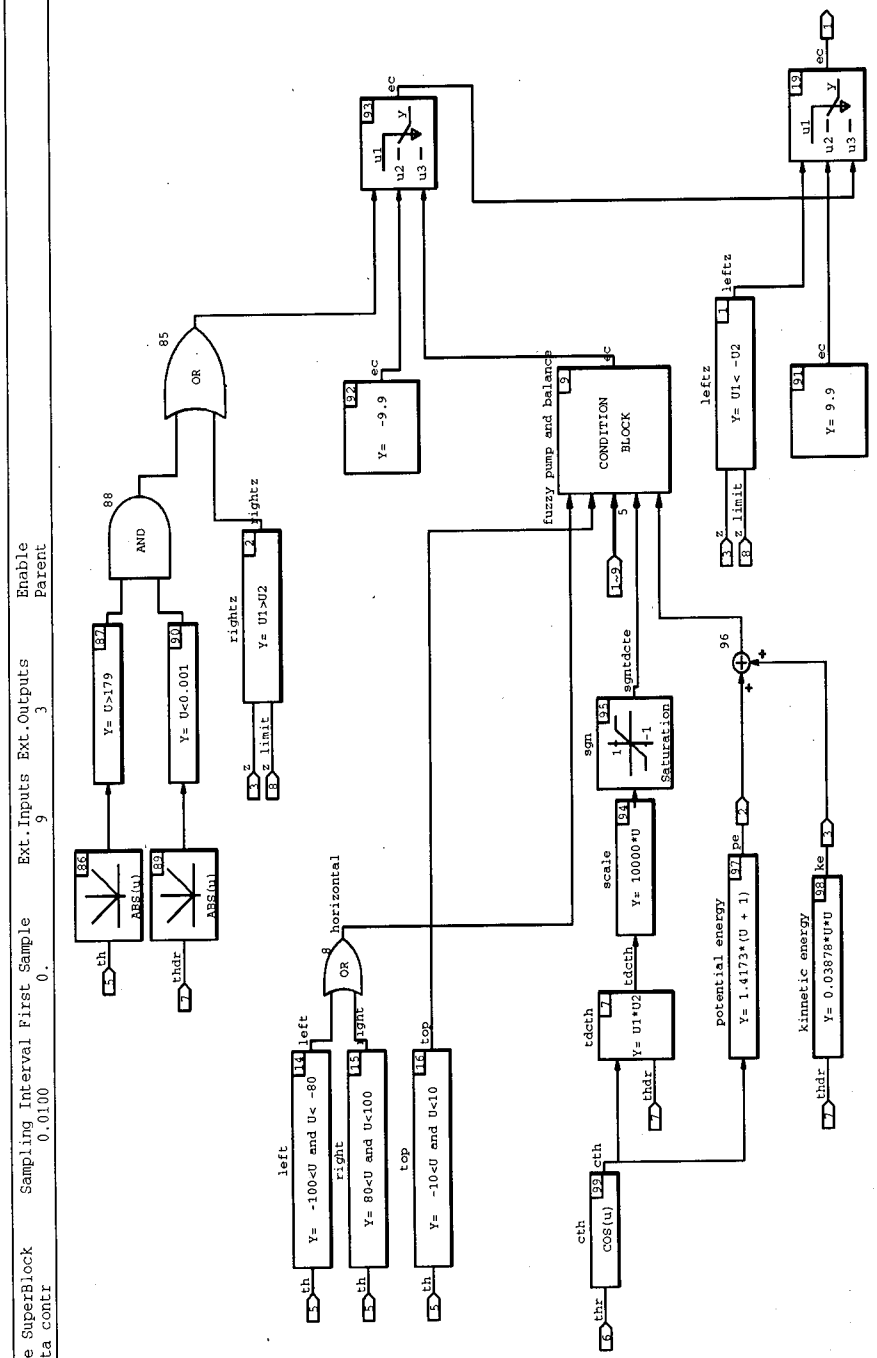

Figure 3-5 Angle

Chapter 4

Results

4.1 Balance and Center

The two loop balancing and centering controller with the friction compensation showed very good results based on near zero initial conditions. It resulted in steady state angular variations of approximately 1.2 degrees either side of the vertical. The cart remained within 3 centimeters of track center. In addition, the control effort was never more than 5 V based on a maximum possible exertion of 10 V. The output response plots are shown in Figure 4-1 and Figure 4-2 where th=θ and thd=θ_d.

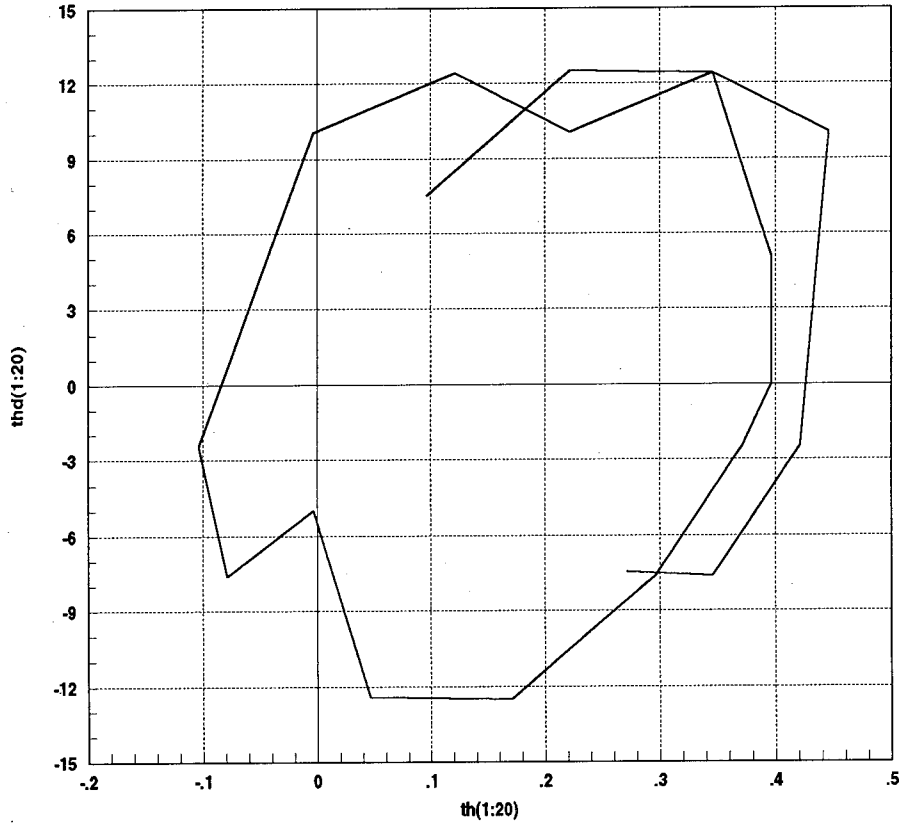

Figure 4-1 Balance and Center Angular Phase Plane

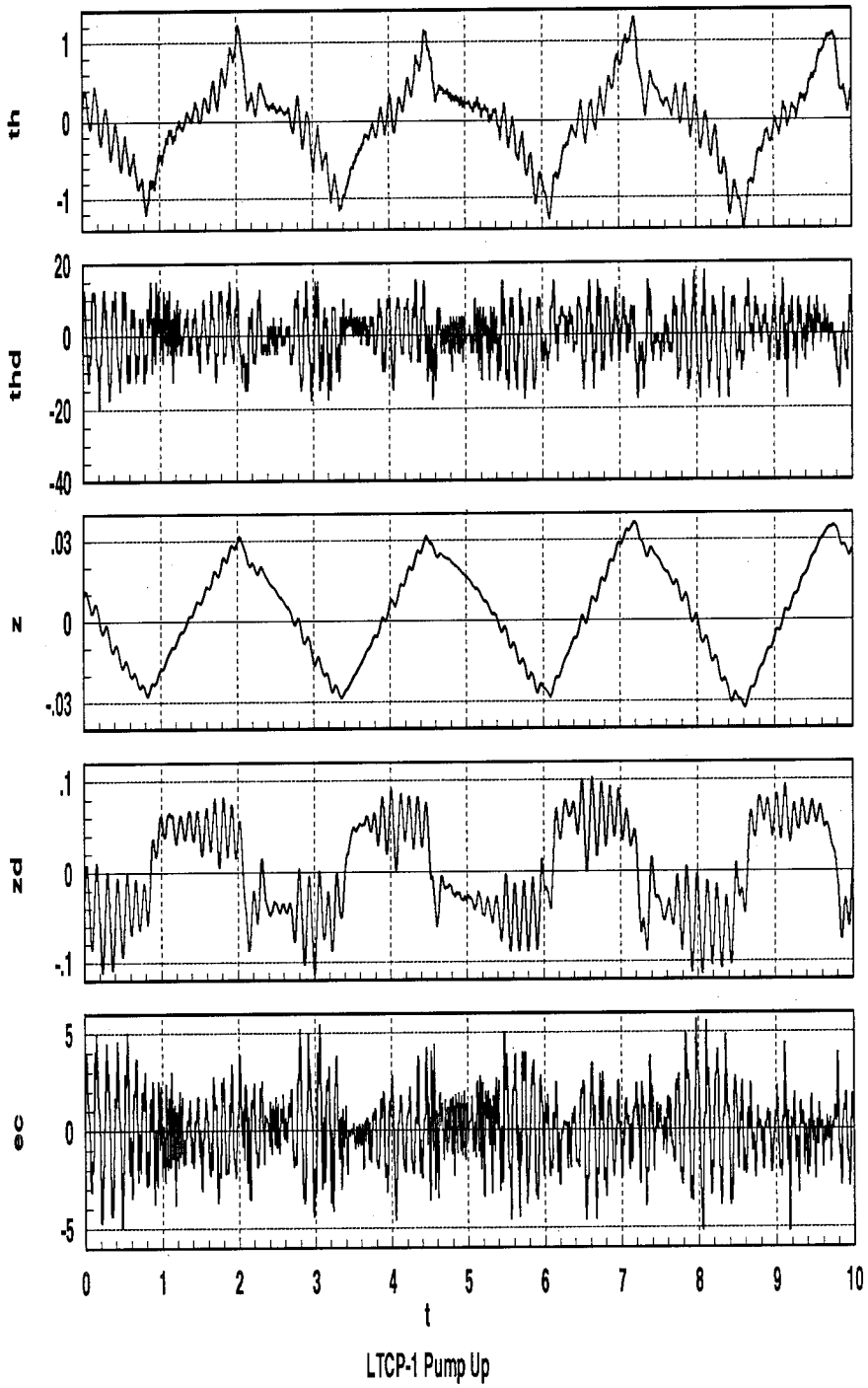

Figure 4-2 Balance and Center Time Response

4.2 Adding and Subtracting Energy for Pump Up

The standard initial condition for the pendulum is hanging straight down at 180 degrees and not swinging at all. Balancing the pendulum from this state is the classic pump up problem. Starting from zero, the controller must add the appropriate amount of energy to the system. Figure 4-3 and Figure 4-4 depict the controller's response to this scenario.

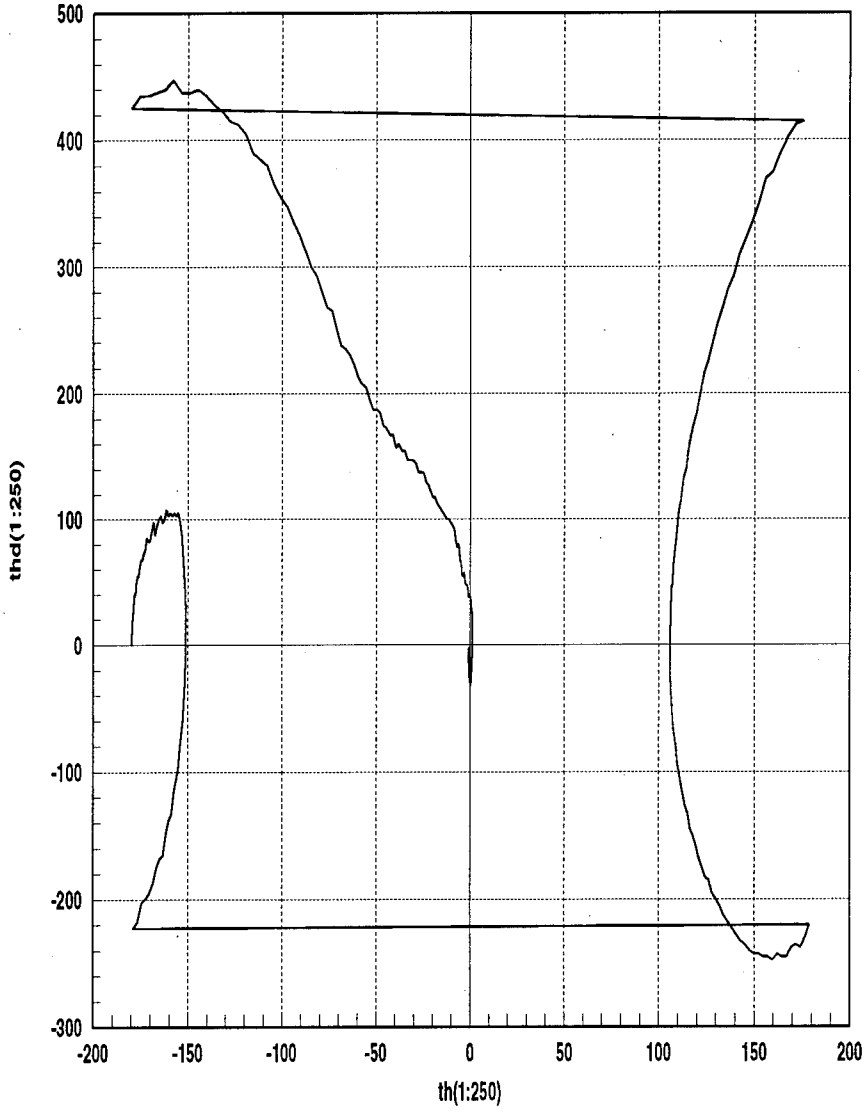

Figure 4-3 Pump Up Angular Phase Plane

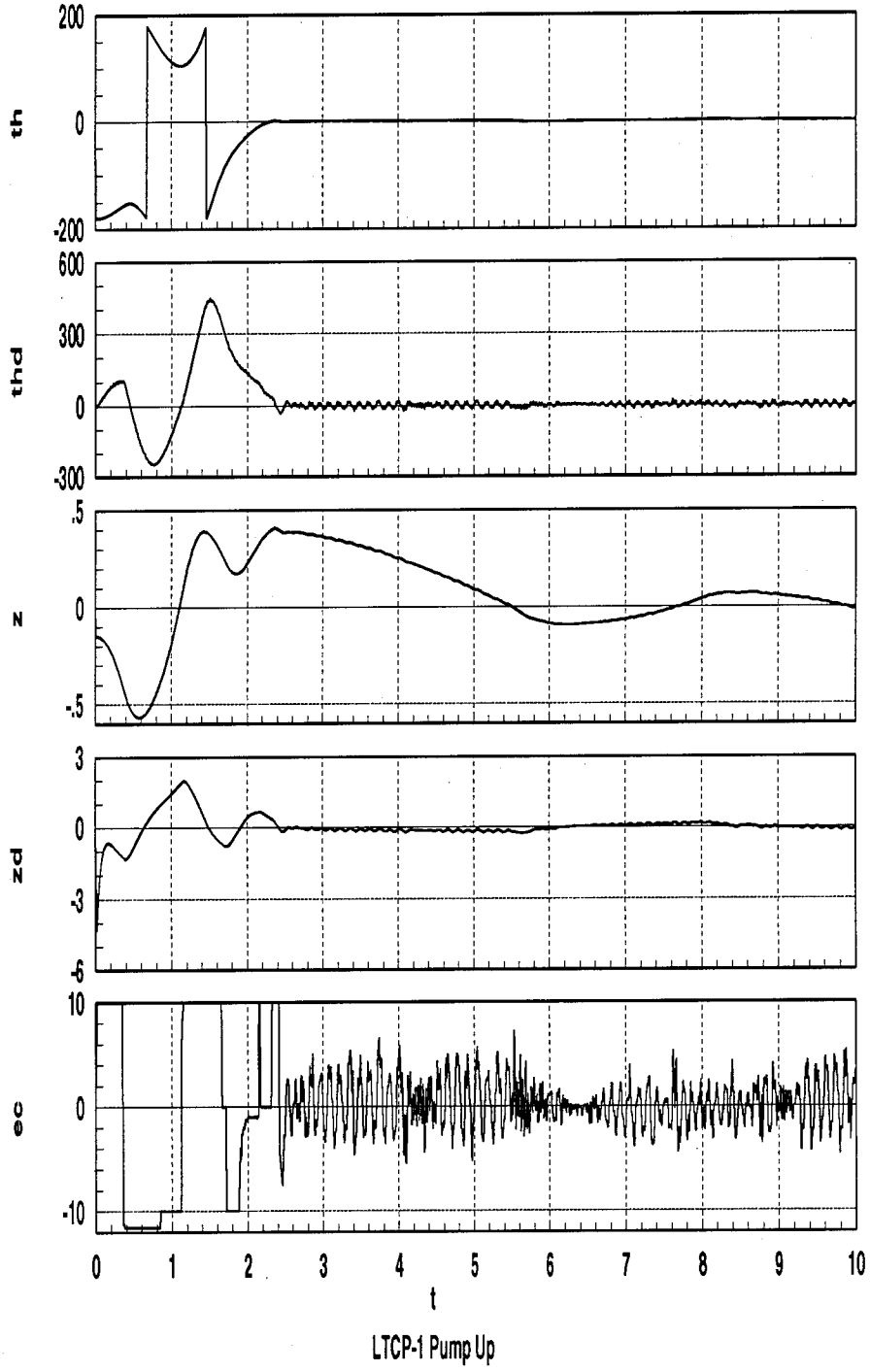

Figure 4-4 Pump Up Time Response

The vertical lines in the θ time response indicate that the angle passed through +/ - 180 degree. To balance the pendulum, the controller initially moved the cart to the left, causing the pendulum to swing up to the right. Approaching the limit of the rail, it then moved cart back to the right, causing the pendulum to accelerate clockwise. This occurred at about 0.4 seconds. Approaching the right limit of the rail, the cart had to accelerate back to the left at 1.2 seconds. The pendulum passed through the horizontal at about 1.7 seconds, and the cart began accelerating back to the right to continue adding energy. By 2.2 seconds, the pendulum was balanced in the vertical position. The cart centered itself by about 5.5 seconds. Although not designed to be minimum time, the 2.2 second pump up is very near the optimum 2.16 second neural network controller developed for the LCTP-1 by Janet Bartlett[2].

To illustrate the robustness of the controller to different sets of initial conditions, the next response is based on a system with too much initial energy. The angle is arbitrary and the pendulum is swinging at a high angular velocity. To balance the pendulum, the controller must remove more than half of the system's total energy. The results are shown in Figure 4-5 and Figure 4-6.

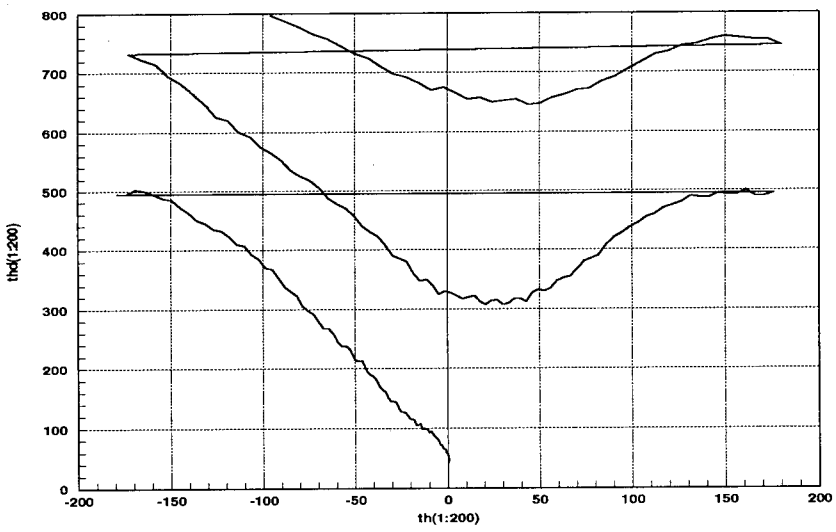

Figure 4-5 Energy Removal Angular Phase Plane

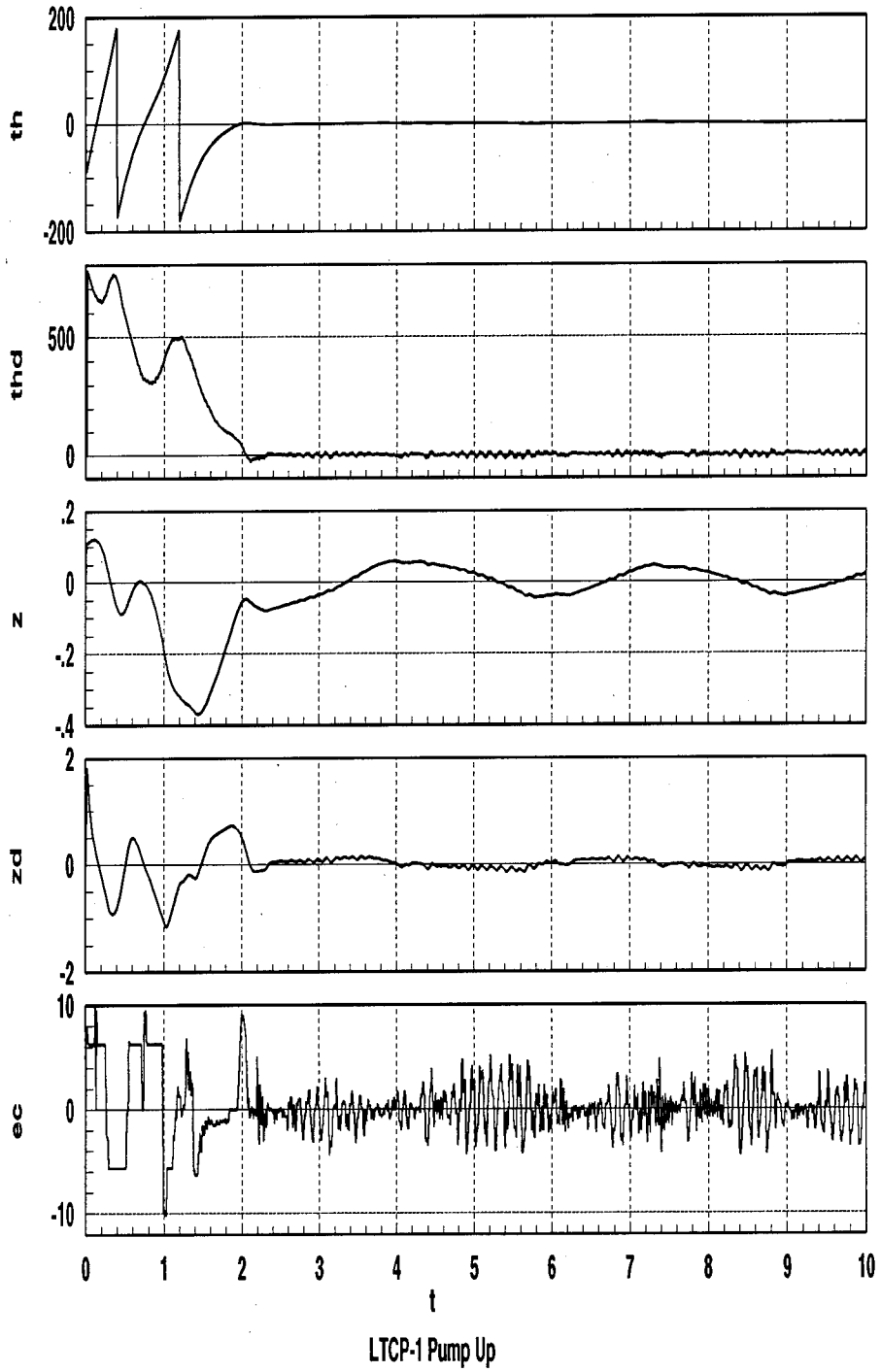

Figure 4-6 Energy Removal Time Response

In this case the angular rate time response is very illustrative. The pendulum is initially swinging with an angular velocity of about 800 deg/sec. In about two seconds, the controller is able to reduce this to nearly 0 deg/sec and balance the pendulum. The cart is back in the center of the track in under 3.5 seconds. To see how the controller is removing energy from the system, look at the time response plots at one instant in time. At 0.8 seconds, the pendulum angle is between 0 and 90 degrees, placing it in the first quadrant. The angular rate is about 350 degrees per second in the positive direction. To take energy out, the cart must accelerate to the left. The high positive control voltage is indeed causing it to accelerate to the left as indicated by the negative slope of the cart velocity profile seen in Figure 4-6.

These two responses show that the controller adjusts itself so as to balance the pendulum, whether it must add or subtract energy. Essentially, it functions regardless of the initial conditions. It therefore meets the primary objective of the research.

4.3 Disturbance Rejection

A very interesting attribute of this fuzzy controller is that it makes the LCTP-1 a self sufficient system. When the controller is turned on, it will maintain the pendulum in the balanced position, regardless of external disturbances. If a person hits the pendulum hard enough so balance cannot be maintained given the system constraints, then the controller will simply allow the pendulum to fall and then catch it the next time it goes through the vertical. Usually a single rotation is sufficient. The plot in Figure 4-9 shows the system initially in a balanced state. Then at about 2.3 seconds, it is hit with an unrecoverable disturbance. Recognizing this, the controller simply lets the pendulum fall and catches it on the way back up. At about 9.25 seconds, it is hit with another disturbance this one is not as large, so that the controller at first attempts to maintain balance. In doing so it nears the edge of the rail and must let it go. Again, the pendulum swings around and the controller catches it on the upswing. The phase plane plots in Figure 4-7 and Figure 4-8 show how the controller moves the angular phase trajectory towards the origin.

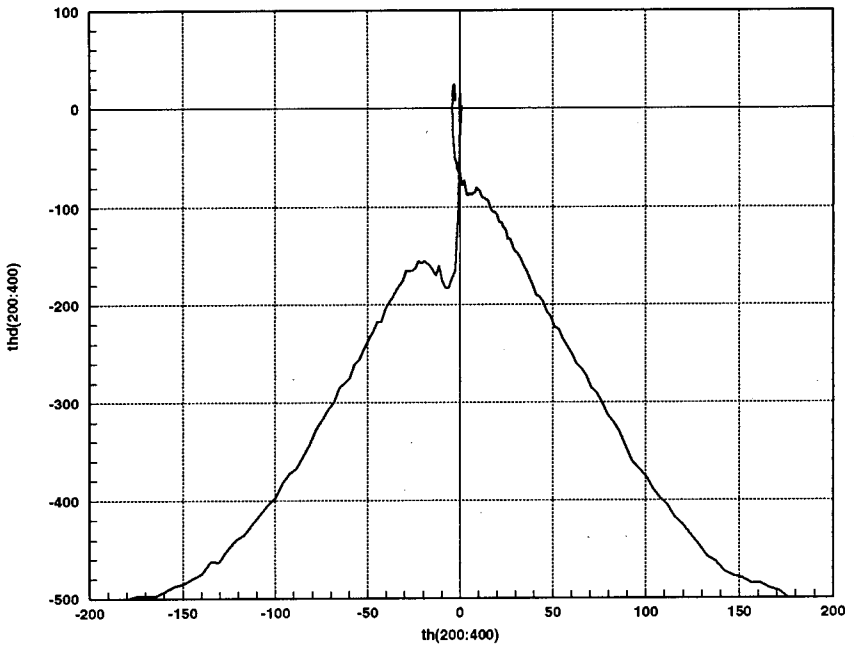

Figure 4-7 Disturbance Rejection (1) Angular Phase Plane

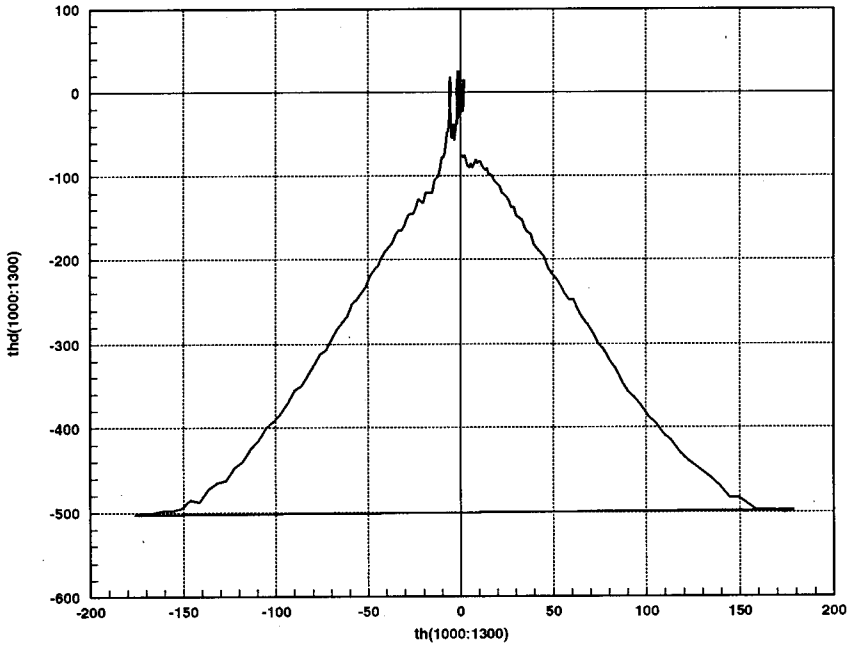

Figure 4-8 Disturbance Rejection (2) Angular Phase Plane

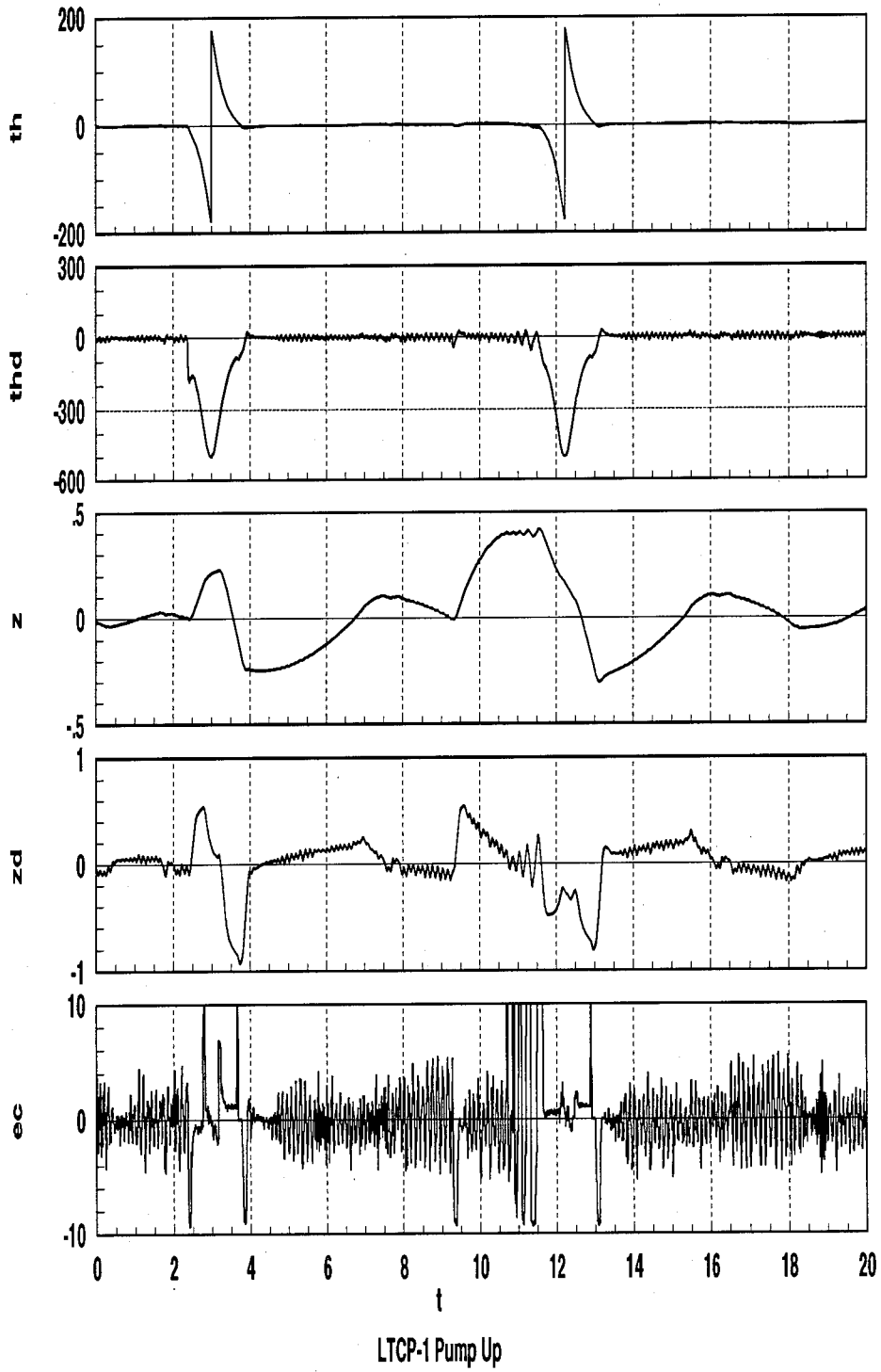

Figure 4-9 Disturbance Rejection Time Response

Chapter 5

Discussion

5.1 Conclusions

The purpose of this work was to develop a controller that could perform the highly discontinuous and nonlinear task of balancing the inverted pendulum from an arbitrary set of initial conditions. Fuzzy logic was chosen as the control technique because of its ability to deal with nonlinear systems, as well as its intuitive nature. The rule base depends on intuition and logic, rather than an exact mathematical model. This makes it more robust to changes in the model, and also gets rid of the need to solve nonlinear differential equations or optimality conditions. Using a set of fuzzy logic controllers, linked in the right way, the primary research objectives were accomplished. In addition, the adjustable desired energy allows for different tip masses and arm lengths to be controlled equally as well with a simple number adjustment on the interactive animation window. This makes the controller very robust.

5.2 Recommendations for Future Study

There are many options for future research on the inverted pendulum using fuzzy logic. The current controller could be improved by further adjustment of the membership functions. This adjustment could be performed manually by experimenting and checking the results. An optimization routine using Genetic Algorithms could also be used. This would involve letting the computer run simulations and compare results automatically. The pump up could be improved so that it would not overshoot the desired energy, which occasionally occurred in experiments. This would be done by simply increasing the number of classes into which the total energy was fuzzified. This increases the size of the pump up rule base and gives the controller better resolution.

A logical next step in the research for the pendulum, is a controller that balances

the dual arm pendulum (LCTP-2). This is a significantly more difficult task, but fuzzy logic has shown excellent potential. Because this is a more sensitive and non-linear task than dealing with the single pendulum, the resolution problems present in the SystemBuild Fuzzy Logic Tool Box have to be rectified.

The problem is that all of the data defined in any fuzzy block must be defined on the same scale. Since the angles, angular rates, and voltages are different by orders of magnitude, defining the membership functions on the same range does not make sense. If unlimited points could be used to define the membership curves, this would be less of a problem, but the more points used, the longer the computation time. A longer computation time results in larger sampling intervals. The scaling problem was partially circumvented by scaling the data before the controller so that they were all on the same magnitude range. This however, made bookkeeping difficult and would better be addressed either by a more flexible fuzzy tool box, or by programming the fuzzy logic code directly. The latter would be the most efficient and flexible path. It could be easily implemented through the user code blocks in SystemBuild.

Bibliography

1 Abramovitch, D. "Some Crisp Thoughts on Fuzzy Logic." Proceedings of the American Control Conference. Baltimore, Maryland, June 1994.

2 Bartlett, J. "Time-Optimal Control of Nonlinear Systems Using Neural Networks." MS Electrical Engineering Thesis, University of Washington, Seattle, Washington 1993.

3 Benson, R., W. E. Schmitendorf, and O. Shaw. "Using Genetic Algorithms for Controller Design: Simultaneous Stabilization and Eigenvalue Placement in a Region." AIAA-92-4465-CP, 1992: 757-761.

4 Bertram, T., F. Svaricek, and H. Schwarz, Institut fur Mess-, Steuer-und Regelungstechnik, University of Duisburg, Postfach 10 15 03, W-4100, Duisburg, Germany

5 Deshpande, S.M., R.R. Kumar, and H. Seywald "A Genetic Algorithm Approach to Solving Optimal Control Problems with Linearly Appearing Controls." AIAA-92-4404-CP, 1992: 750-756.

6 Dubois D. and H. Prade Fuzzy Sets and Systems. Theory and Applications. Academic Press: Orlando, Florida, 1980.

7 Fogel, D. Evolutionary Optimization. Orincon Corporation, San Diego California.

8 Geva, S. and J. Sitte. "A Cartpole Experiment Benchmark for Trainable Controllers." IEEE Control Systems. Oct 1993: 40-51.

9 Goldberg, D. Genetic Algorithms in Search, Optimization, and Machine Learning. New York: Addison-Wesley Publishing Company Inc., 1989.

10 Han, J.Y., and V. McMurray. "Two-Layer Multiple Variable Fuzzy Logic Controller." IEEE Transactions on Systems, Manipulation, and Cybernetics. Vol 23, No 1, Jan/Feb 1993: 277-285.

11 Hung, C.C. and B. Fernandez, "Comparative Analysis of Control Design Techniques for a Cart-Inverted Pendulum in Real-Time Implementation," Proc. of the American Control Conference, San Fransisco, CA, June 1993.

12 Integrated Systems, Inc. "SystemBuild User Guide." Santa Clara, California, 1992.

13 Integrated Systems, Inc. "Matrix-x User Guide." Santa Clara, California, 1992.

14 Katai, O., T. Sawaragi, S. Iwai, Skohno and T. Kataoka, "Constraint-Oriented Fuzzy Control Schemes for Cart-Pole Systems by Goal Decoupling and Genetic Algorithms." Fuzzy Control Systems, ed A. Kandel and G. Langholtz, CRC Press, Tokyo, 1994.

15 Kawaji, S., T. Maeda, and N. Matsunaga. "Learning Control of an Inverted Pendulum Using Neural Networks." Proceedings of the 31st Conference on Decision and control. Tuscon, Arizona, December 1992.

16 Khanna, T. Foundations of Neural Networks. Reading, Massachusetts: Addison-Wesley Publishing Company, 1990.

17 Krishna Kumar, K. "Genetic Algorithms: An Introduction and an Overview of Their Capabilities." AIAA-92-4462-CP, 1992: 728-734.

18 Kristinsson, K., and G.Dumont. "System Identification and Control Using Genetic Algorithms." IEEE Transactions on Systems, Manipulation, and Cybernetics. Sep 1992: 1033-1046.

19 Kuschewski, J. , S. Hui, and H. Zak. "Applications of Feedforward Neural Networks to Dynamical System Identification and Control." IEEE Transactions on Control Systems Technology. Mar 1993: 37-49.

20 Lin, Y.J. and T.S. Lee. "Modeling for Fuzzy Logic Control of Deformable Manipulators." Proceedings of the American Control conference. San Francisco, California, June 1993.

21 Mauer, G. Computer-Supported Controller Design with Model-Based and Fuzzy-Logic Methods. Unpublished Paper. University of Nevada, Las Vegas, Nevada.

22 Miller, T., R. Sutton, and P. Werbos, ed. Neural Networks for Control. Cambridge, Massachusetts: MIT Press, 1990.

23 Ostertag, E., and M.J. Carvalho-Ostertag. "Fuzzy Control of an Inverted Pen-

dulum with Fuzzy Compensation of Friction Forces." Int. J. Systems Sci., 1993, Vol 24, no 10: 1915-1921.

24 Reinhardt, M. Physics of neural Networks, Neural Networks and Introduction. Berlin: Springer-Verlag, 1990.

25 Sepp, K. "Robust Control of Linear Track Cart-Pendulum." MS Electrical Engineering Thesis, University of Washington, Seattle, WA 1994.

26 Seywald, H., R.R. Kumar, and S.M. Deshpande. A Genetic Algorithm Approach to Solving Optimal Control Problems with Linearly Appearing Controls. Analytical Mechanics Associates, Inc. Hampton: 1992.

27 Wiklund, M., A. Kristenson, and K.J. Astrom. "A New Strategy for Swinging Up an Inverted Pendulum." Proceedings of the 12th Triennial World Congress. Sydney, Australia, 1993.

28 Yamakawa, T. "Stabilization of an Inverted Pendulum by High Speed Fuzzy Logic Controller Hardware System." Fuzzy Sets and Systems, Vol 32, 1989.

29 Zhang, W. "Two Stage Inverted Pendulum" FIDE Application Note 008-921014, Aptronix Inc. 2150 North First Street #300, San Jose CA 95131, 1992.

Appendix A

System Dynamics and Modeling

A.1 Cart/Pendulum Dynamics

The cart/pendulum system is modeled based on the conventions diagrammed in Figure A-1.

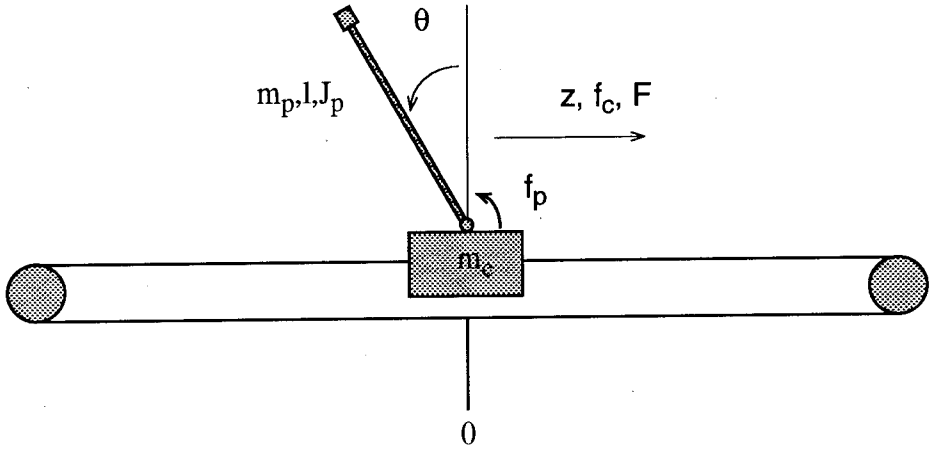

Figure A-1: Model of the Cart and Pendulum

where:

mp = mass of the pendulum (kg)

l = distance from the pendulum center of mass (COM) to the pivot point on the cart (m)

Jp = pendulum moment of inertia about its center of mass (kgm^2)

mc = mass of the cart (kg)

F = force exerted on the cart by the belt (N)

fp = friction in the pendulum joint (N)

fc = friction between the cart and the track (m/sec^2)

There are many possible approaches that can be used to arrive at a proper mathematical model. The most common use either an energy based analysis or a Newtonian momentum based analysis. The inverted pendulum is ideally suited to the energy based approach, and the Lagrangian formulation is the one used in the model development depicted here.

The Lagrangian function L is defined as

$$L = T_{total} - V_{total} \qquad (A\text{-}1)$$

where T_{total} is the system kinetic energy and V_{total} is the system potential energy.

The LCTP-1 has two degrees of freedom, the pendulum rotation angle (θ) and the cart translation position (z). These two variables define the generalized coordinates for the formulation of Lagrangian equations of motion. The system of equations is given by

$$\frac{d}{dt}\left(\frac{\partial L}{\partial \dot{z}}\right) - \frac{\partial L}{\partial z} = Q_z \qquad (A\text{-}2)$$

$$\frac{d}{dt}\left(\frac{\partial L}{\partial \dot{\theta}}\right) - \frac{\partial L}{\partial \theta} = Q_\theta \qquad (A\text{-}3)$$

where Q_z and Q_θ are the non-conservative generalized forces in z and θ.

A.1.1 Lagrangian Function

The first step in the Lagrangian formulation of the equations of motion is to determine the kinetic and potential energies. This allows us to define the Lagrangian function in terms of the system parameters.

The kinetic energy of the system is given by

$$T_{total} = T_{cart} + T_{pendulum} \tag{A-4}$$

where

$$T_{cart} = \frac{1}{2} m_c \dot{z}^2 \tag{A-5}$$

and

$$T_{pendulum} = \frac{1}{2} J_p \dot{\theta}^2 + \frac{1}{2} m_p \left[(\dot{z} - l\dot{\theta}\cos\theta)^2 + (l\dot{\theta}\sin\theta)^2 \right] \tag{A-6}$$

The potential energy of the system is given by

$$V_{total} = V_{pendulum} = m_p g l \cos\theta \tag{A-7}$$

where g is the gravitational acceleration in m/sec^2.

Substituting (*A-6*) and (*A-7*) into (*A.1*) results in the Lagrangian function in terms or z and θ.

$$L = \frac{1}{2} J_p \dot{\theta}^2 + \frac{1}{2} m_p \left[(\dot{z} - l\dot{\theta}\cos\theta)^2 + (l\dot{\theta}\sin\theta)^2 \right] - m_p g l \cos\theta \tag{A-8}$$

A.1.2 Non-conservative Forces

The non-conservative forces are those which add or subtract from the system's total energy. In this case the frictional forces take from the total energy and the actuator adds to the total energy. There is friction acting at the pendulum joint (f_p) as well as between the cart and the rail (f_c). The sign conventions are illustrated in Figure A.1.

They may be characterized as follows

$$f_c = (-\upsilon \dot{z} - f_s) \tag{A-9}$$

where υ is coefficient of sliding friction and f_s is a combination of the static and coulomb friction.

$$f_p = -C\dot{\theta} \tag{A-10}$$

where C is the coefficient of viscous friction in the joint.

The force that the actuator applies to the cart is F defined later.

$$Q_z = F - \upsilon \dot{z} - f_s \tag{A-11}$$

$$Q_\theta = -C\dot{\theta} \tag{A-12}$$

A.1.3 Plant Equations of Motion

Substituting equations *(A.8)*, *(A.11)*, and *(A.12)* into *(A.2)* and *(A.3)* results in the following dynamic equations:

$$(m_c + m_p)\ddot{z} + m_p l\dot{\theta}^2 \sin\theta - m_p l\ddot{\theta}\cos\theta = F - \upsilon \dot{z} - f_s \tag{A-13}$$

$$m_p l^2 \ddot{\theta} - m_p l\ddot{z}\cos\theta + J_p\ddot{\theta} - m_p g l \sin\theta = -C\dot{\theta} \tag{A-14}$$

These two second order, nonlinear differential equations describe the dynamics of the inverted pendulum in response to a force F applied at the cart.

A.2 Actuator Dynamics

The actuator is a direct current (DC), permanent magnet, brush type servo motor. It is modeled as an ideal electromechanical device as depicted in Figure A-2.

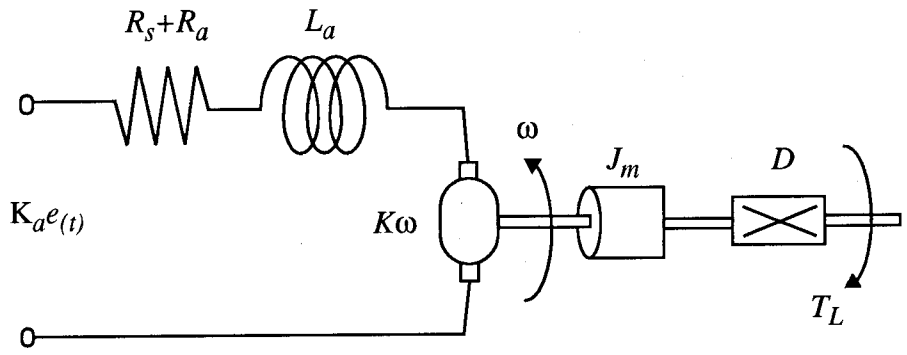

Figure A-2 Motor Model

This model results in actuator dynamics that can be characterized by

$$K_a e(t) = (R_s + R_a) i_a + L_a \frac{di_a}{dt} + K\omega \qquad (A\text{-}15)$$

$$Ki_a = J_m \frac{d\omega}{dt} + D\omega + T_L \qquad (A\text{-}16)$$

where K_a = Servo Amplifier Gain (V/V)

$e(t)$ = Amplifier Voltage Input (V)

R_s = Servo Amplifier Resistance (Ω)

i_a = Motor Armature Current (A)

R_a = Motor Armature Resistance (Ω)

L_a = Motor Armature Current (A)

K = Motor Constant (V/rad/sec)

ω = Motor Rotational Velocity (rad/sec)

J_m = Motor and Drive Train Moment of Inertia (kg m^2)

D = Coefficient of Viscous Friction (N/rad/sec)

T_L = Load Torque (Nm)

5.30 Nonlinear System Model

The full system model is a combination of the plant and actuator dynamics. The torque output by the motor must be related to a force applied on the cart, and then substituted into the plant equations. The torque is converted to a force through the pulley using the following relationship

$$T_L = Fr \qquad (A\text{-}17)$$

where r = radius of the drive pulley (m).

The motor rotational velocity, ω, can be related to the linear velocity of the cart

$$\omega = \frac{\dot{z}}{r} \qquad (A\text{-}18)$$

Thus, making the necessary substitutions leads to the complete set of nonlinear equations describing the LCTP-1 system dynamics

$$(m_c + m_p)\ddot{z} + m_p l\dot{\theta}^2 \sin\theta - m_p l\ddot{\theta}\cos\theta = F - \upsilon\dot{z} - f_s \qquad (A\text{-}19)$$

$$(J_p + m_p l^2\ddot{\theta}) - m_p l\ddot{z}\cos\theta + J_p\ddot{\theta} - m_p g l\sin\theta = -C\dot{\theta} \qquad (A\text{-}20)$$

$$K_a e(t) = (R_a + R_s) i_a + L_a \frac{di_a}{dt} + K\frac{\dot{z}}{r} \qquad (A\text{-}21)$$

$$Ki_a = \frac{J_m}{r}\ddot{z} + \frac{D}{r}\dot{z} + Fr \qquad (A\text{-}22)$$

Table A-1 Parameter Values

Parameter	Value
m_p	0.324 (kg)
l	0.445 (m)
J_p	0.008 (kg m^2)
m_c	2.3 (kg)
g	9.81 (m/s^2)
υ	5.0 (kg/sec)
C	0.0022 (N/sec)
K_a	3.6 (V/V)
R_s	0.0 (Ω)
R_a	1.3 (Ω)
L_a	0.0033 (H)
K	0.137 (V/rad/sec)
J_m	0.00458
D	0.0021 (N/rad/sec)
r	0.08 (m)

Appendix B

System Hardware Configuration

The LCTP-1 in the UWCSL has the layout shown in figure B-1. The cart pendulum mechanization is simple. The pendulum angle is controlled by moving the cart back and forth along a linear track. The cart is moved along the track using a slotted belt which runs around the pulleys located on either side of the track. The pulley on the left is attached to a DC motor (Appendix A), which performs the actuation. The belt and pulley system convert the torque created by the motor into a linear force acting on the cart.

Feedback information is provided by optical encoders. They are Hewlett Packard HEDS_6010, 3 channel, high resolution, incremental optical encoders with 1024 lines of resolution over 360 degrees. Angle information is supplied by the encoder mounted at the pendulum pivot shaft on the cart. The z position information is provided by another optical encoder attached to the right pulley shaft.

The DELL computer used by the AC100 software, contains all of the necessary input-output hardware. This includes a Digital Signal Processor (DSP) for analog to digital (A/D) conversions and quadrature decoding of the encoder signals. It also includes an IP-DAC which provides six channels of 12-bit digital to analog (D/A) conversion. Channel one works on a +-10V range, and all of the other channels work on a +-5V range.

The GUI communicates with the real-time controller via the ethernet link. This prevents the GUI information from being completely up to date. The network link can get bogged down, slowing the information transfer. The controller does however, run independent of the GUI so that this is not a problem.

For more information see the thesis written by Kalev Sepp[25].

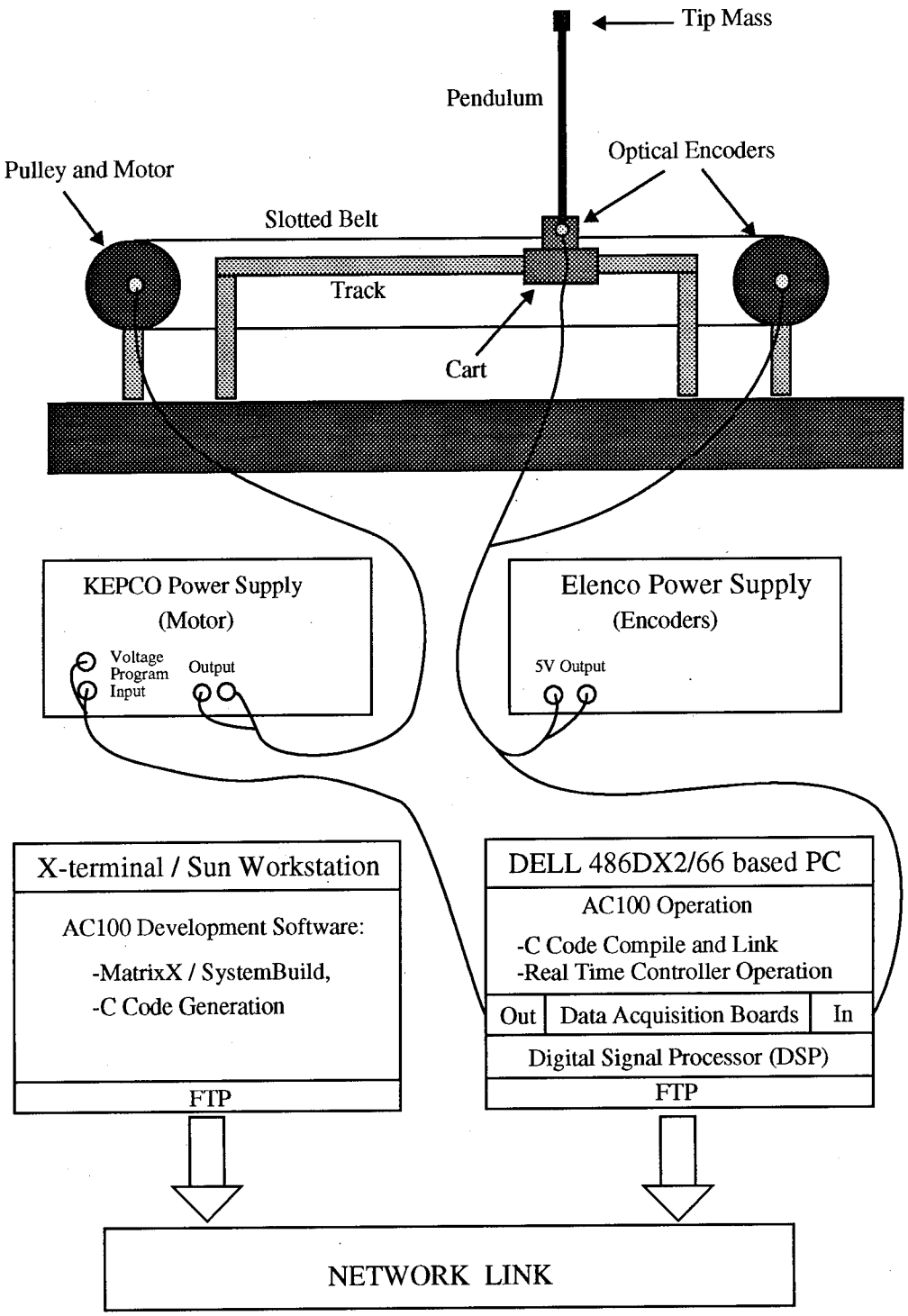

Figure B-1 Hardware Configuration for LCTP-1

Appendix C

Operation Instructions

The fuzzy logic controller developed herein may be run by following these simple step by step instructions.

1. Turn on the Dell 466V personal computer and monitor. They are located right next to the pendulum.
2. Load the network driver on the Dell by typing *ldether* at the DOS prompt.
3. Launch the AC100/C30 server program by typing *ac100svr* at the DOS prompt.
4. Log on to the Capri workstation as user *ac100*. This is usually done remotely on the X-terminal *eagle* as it is nearest the pendulum. In this case the display variable must be set with the command *setenv DISPLAY eagle:0*. If logged on to Capri directly, open the window manager using the command *openwin*.
5. Change directories using the command *cd mike/pump* at the UNIX prompt.
6. Run the AC100 software using the command *ac100* at the UNIX prompt. This will open the AC100 main window which is shown in Figure C-1.
7. For correct encoder initialization, ensure that the cart is in the center of the track and the pendulum is stationary hanging straight down.
8. Turn on the Elenco Precision Power Supply for the optical shaft encoders.
9. Double click on the ac100 main window block *download and run* using the left mouse button. This will bring up the interactive animation window shown in Figure C-2. The DELL should print controller information on the screen.
10. Start the controller with a single click on the *start* block on the control pad at the bottom of the screen. The correct information should now be displayed on the interactive animation window. The angle should be -180 degrees.
11. Turn off the controller using a single click on the cutoff switch at the top left corner of the interactive animation window. The switch should turn from green to red. This is to prevent immediate activation of the controller when the Power Supply is turned on.
12. Ensure that the KEPCO Power Amplifier is configured for voltage control. The

Mode Switch should be to the left and the input from the DELL should be connected to the input jacks on the left side. They are marked "voltage programming input."

13. Turn on the KEPCO Power Amplifier by flipping the power switch on the top left corner.

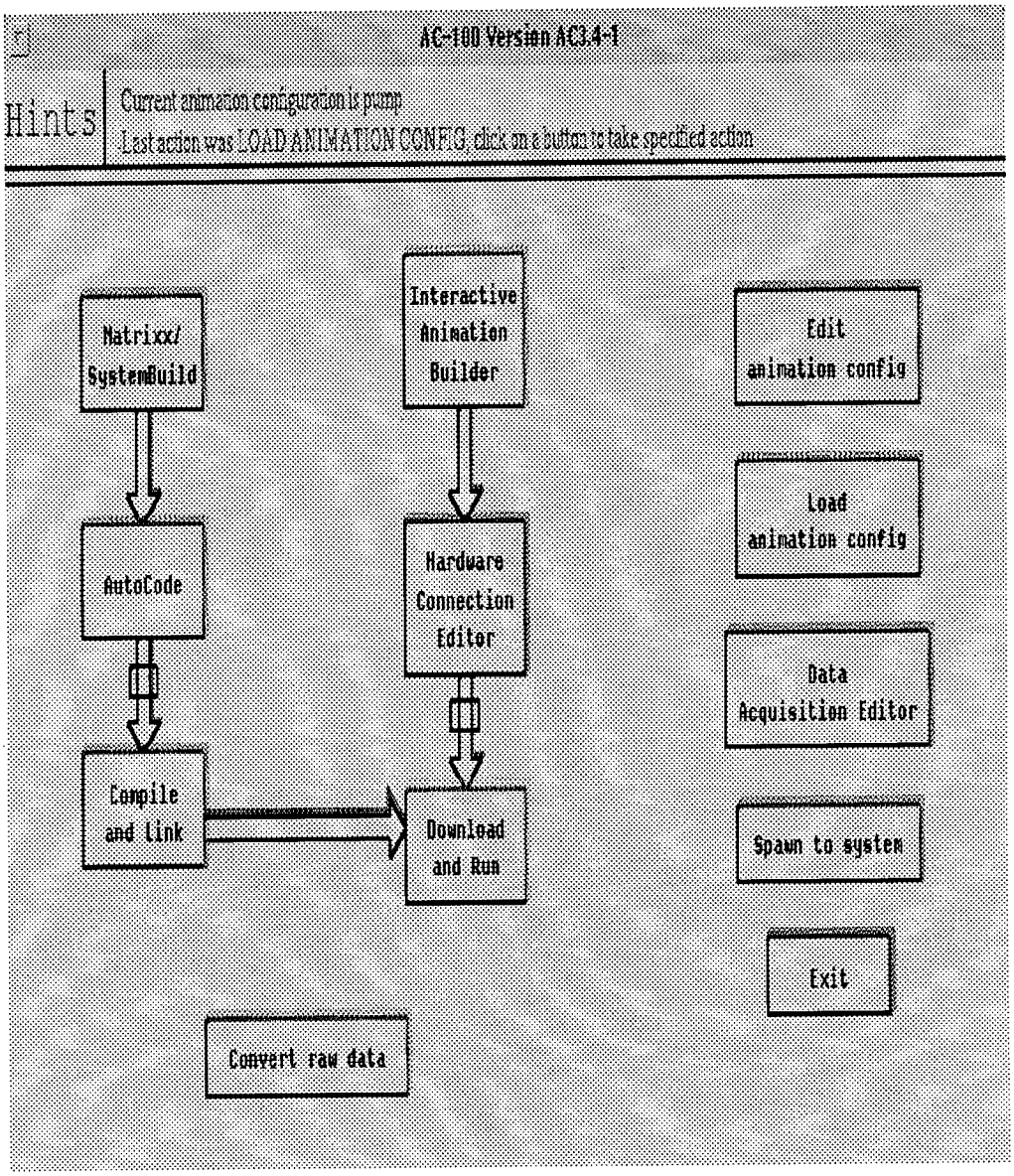

Figure C-1 AC100 Main Window

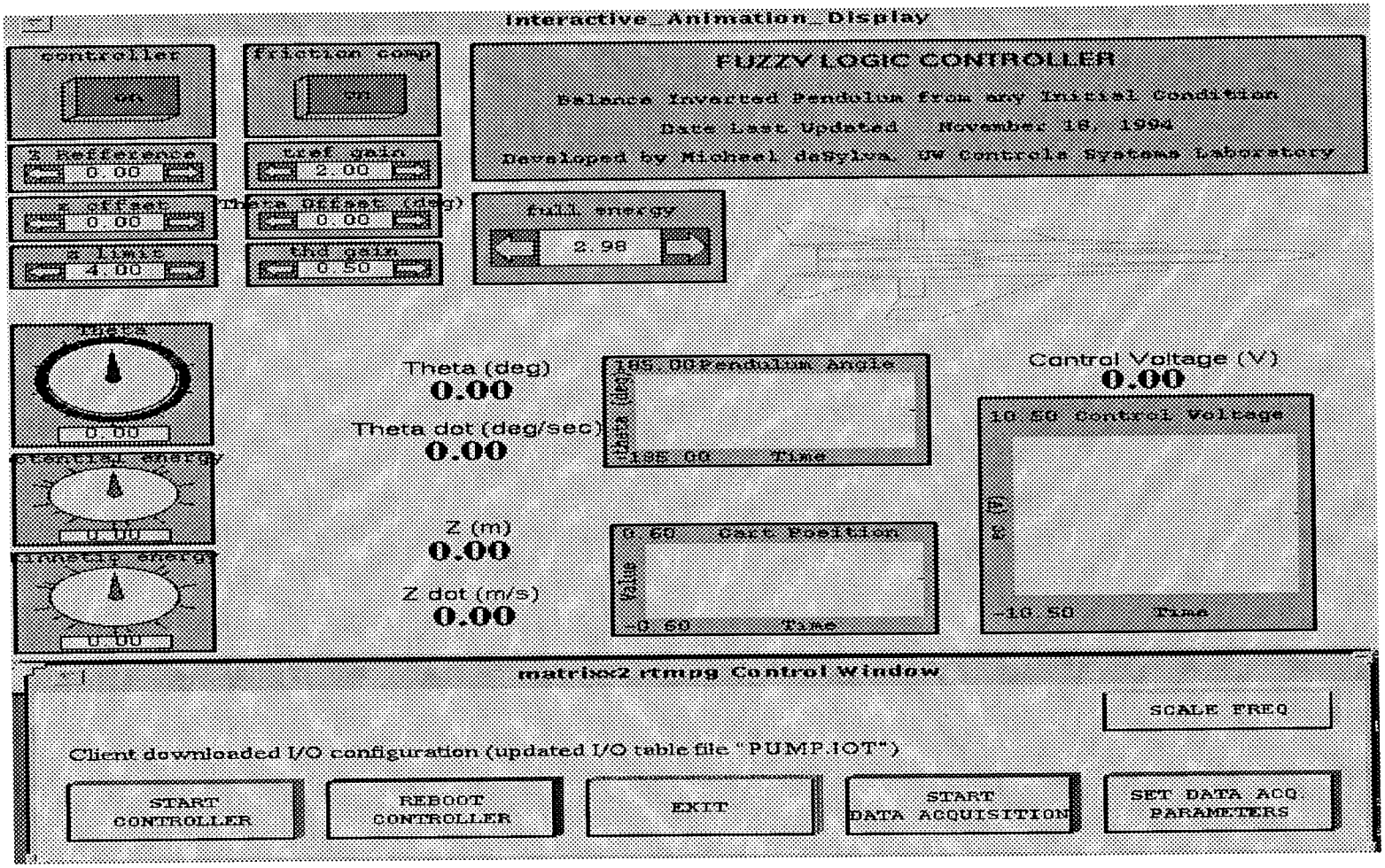

Figure C-2 Interactive Animation Window

Appendix D

SystemBuild Block Diagrams

D.1 Modeling

The MatrixX file contains the system parameters and it was used to simplify the programming of the nonlinear model.

```
C = 0.0022;  // C = coefficient of viscous friction (N/sec)
D = 0.0021;  // D = coefficient of viscous friction (N/rad/sec)
g = 9.807;   // Gravitational acceleration (m/sec^2)
Jp = 0.008;  // Moment of Inertia of Pendulum (kg*m^2)
Jt = 0.00458; // Moment of Inertia of  motor and drive train (kg*m^2)
Ka = 3.6;    // Amplifier gaim (V/V)
Km = 0.137;  // Motor constant (V/rad/sec)
l = 0.445;   // Distance from pendulum center of mass to the pivot (m)
La = 0.0033; // Motor armature inductance (H)
Mp = 0.324;  // Pendulum mass (kg)
Mc = 2.3;    // Cart mass (kg)
r = 0.08;    // Drive pulley radius
Ra = 1.3;    // Motor armature resistance (ohms)
R1 = 0.0;    // Amplifier Resistance (ohms)
v = 5.0;     // Coefficient of sliding friction (kg/sec)

// Constants Defined to Simplify Modeling
C1 = Mp*l/(Mc+Mp);
C2 = Mp*l/(Jp+Mp*(l*l));
C3 = C2*g;
C4 = -C/(Jp+Mp*(l*l));
CC=[C1,C2,C3,C4];
Kzd1=-Km/(La*r);
Kzd2=-D/r/r;
Ki1=-(R1+Ra)/La;
Ki2=Km/r;
Ke=Ka/La;
kzdd1=-Jt/r/r;
```

Figure D-1 Nlpend.mws

Discrete SuperBlock	Sampling Interval	First Sample	Ext.Inputs	Ext.Outputs	Enable
NLPLant	0.0100	0.	1	5	Parent

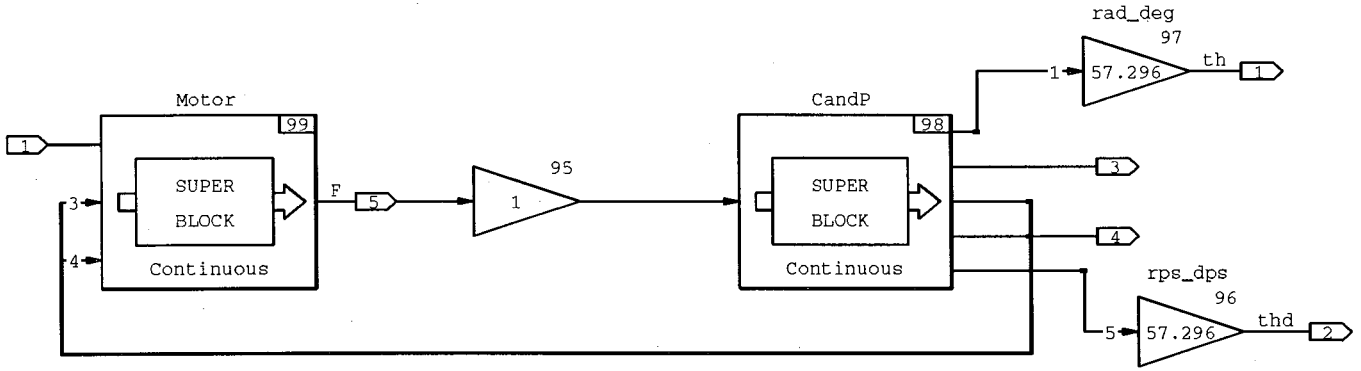

Figure D-2 Nonlinear System Model

Continuous SuperBlock	Ext.Inputs	Ext.Outputs
Motor	3	1

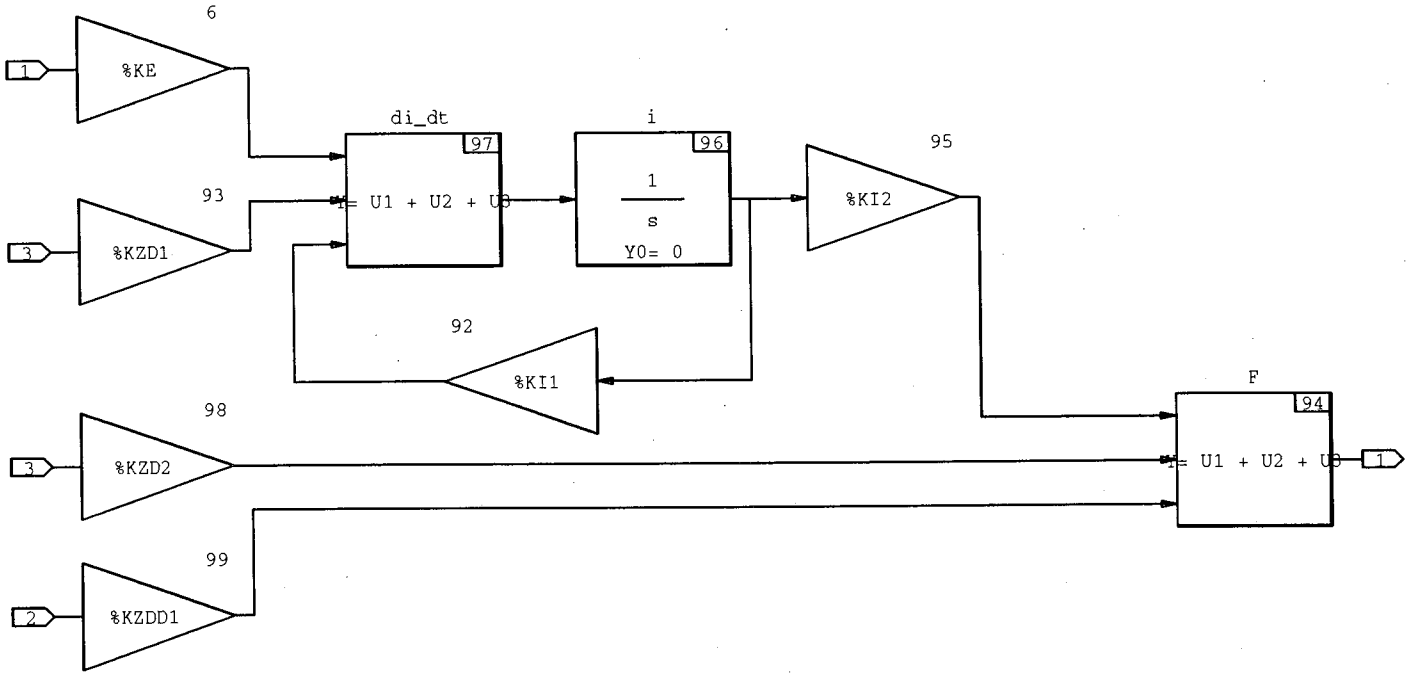

Figure D-3 Motor Model

Continuous SuperBlock	Ext.Inputs	Ext.Outputs
CandP	1	5

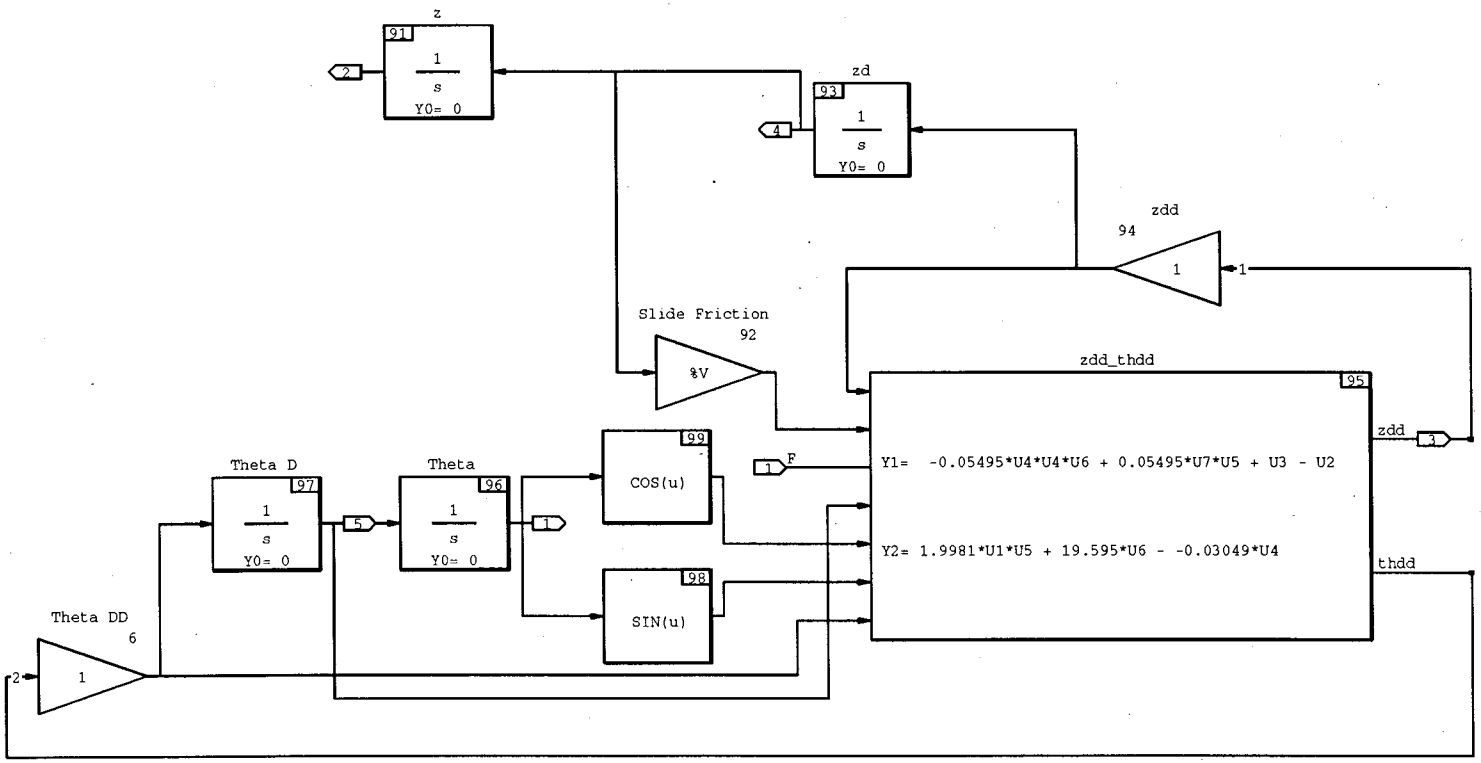

Figure D-4 Nonlinear Cart and Pendulum Model

D.2 Controller Block Diagrams

The following figures depict the actual SystemBuild block diagrams of the controller. It is from these block diagrams that the C code is generated. They are generally ordered from top to bottom on the hierarchy.

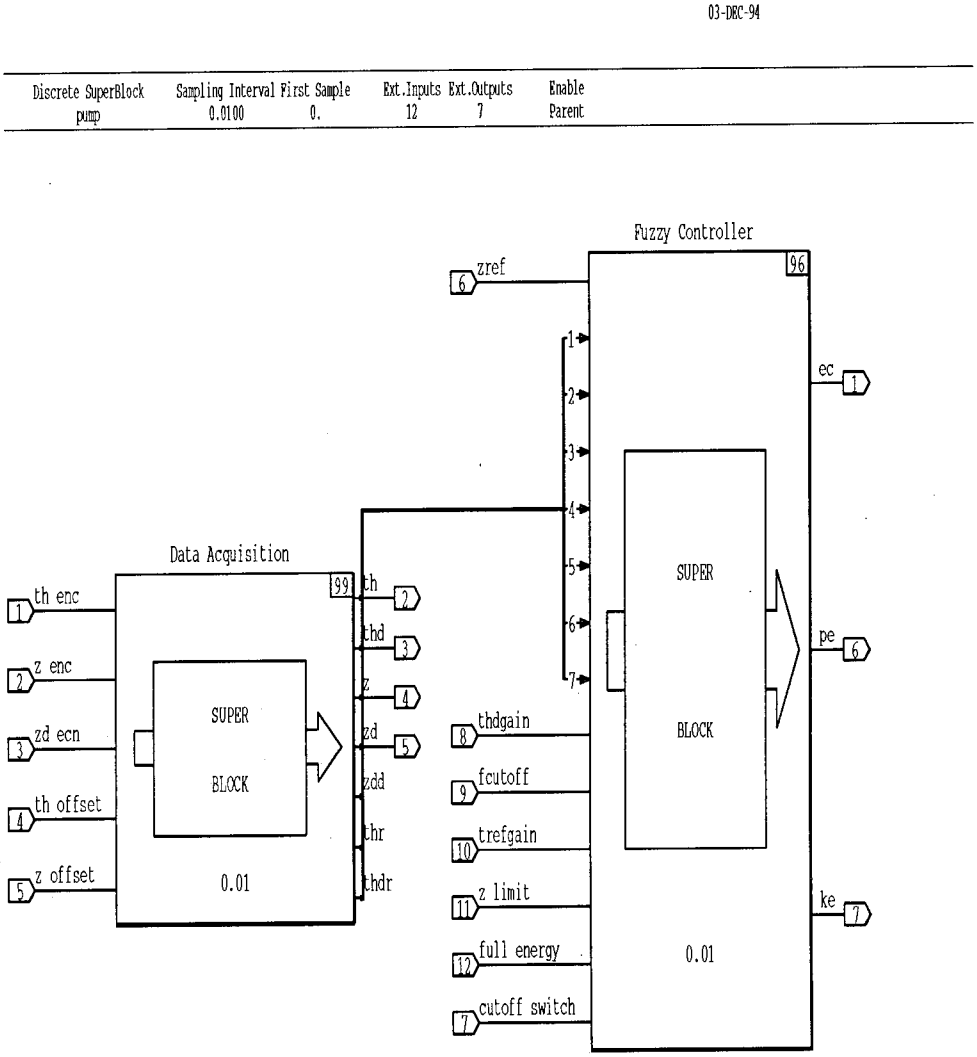

Figure D-5 Controller and Data Acquisition

Discrete SuperBlock	Sampling Interval	First Sample	Ext.Inputs	Ext.Outputs	Enable
Data Acquisition	0.0100	0.	5	7	Parent

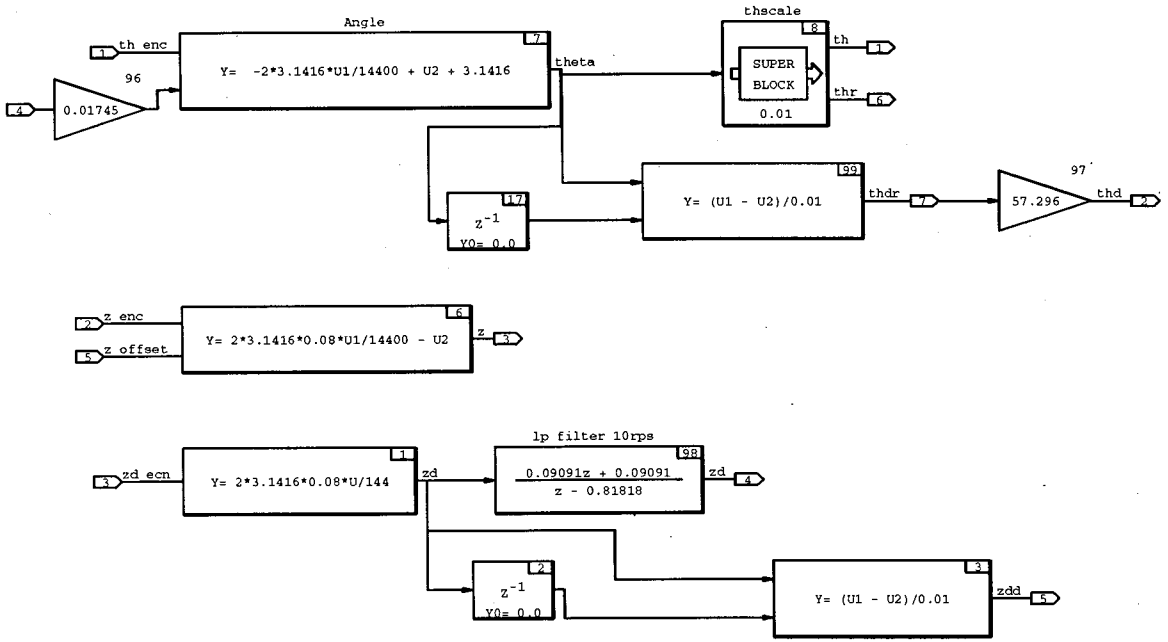

Figure D-6 Data Acquisition

Discrete SuperBlock	Sampling Interval	First Sample	Ext.Inputs	Ext.Outputs	Enable
thscale	0.0100	0.	1	2	None

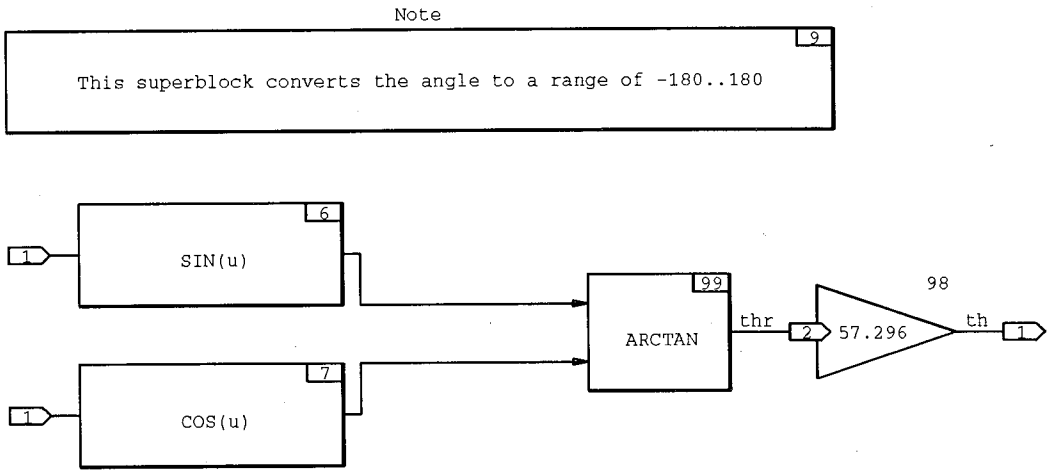

Figure D-7 Theta Range Specification

Discrete SuperBlock	Sampling Interval	First Sample	Ext.Inputs	Ext.Outputs	Enable
Fuzzy Controller	0.0100	0.	14	3	Parent

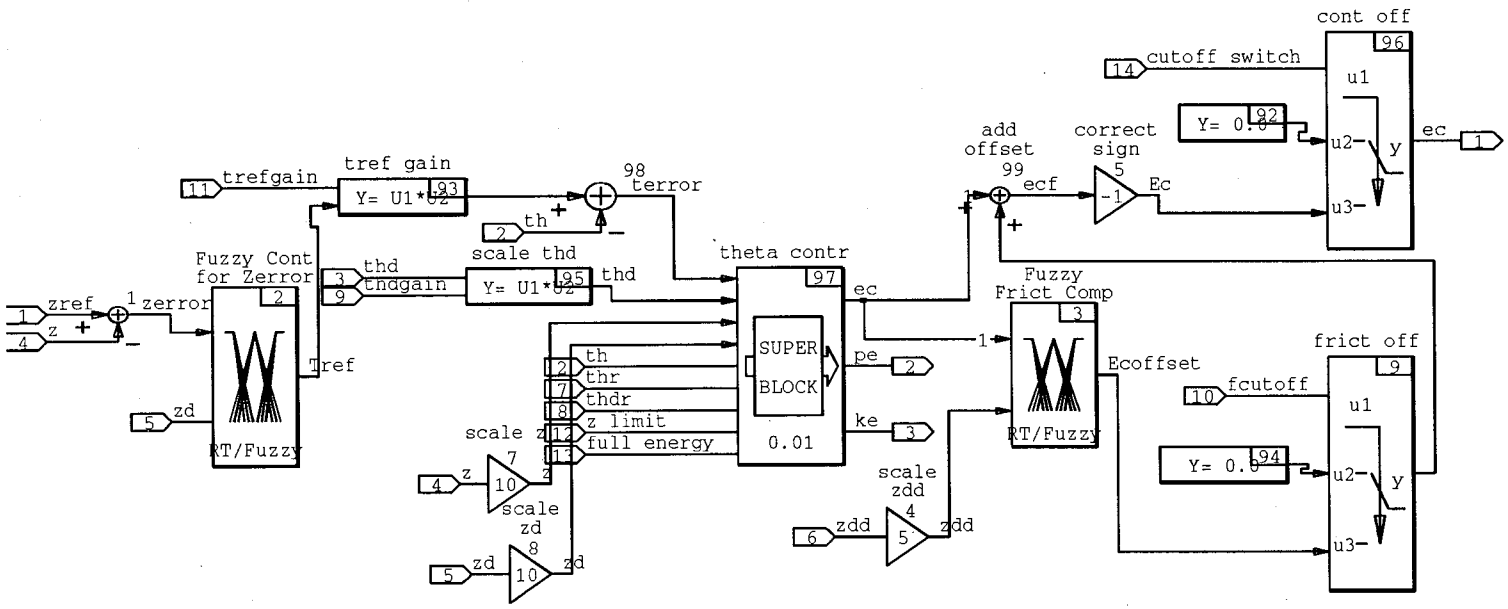

Figure D-8 Full Fuzzy Controller

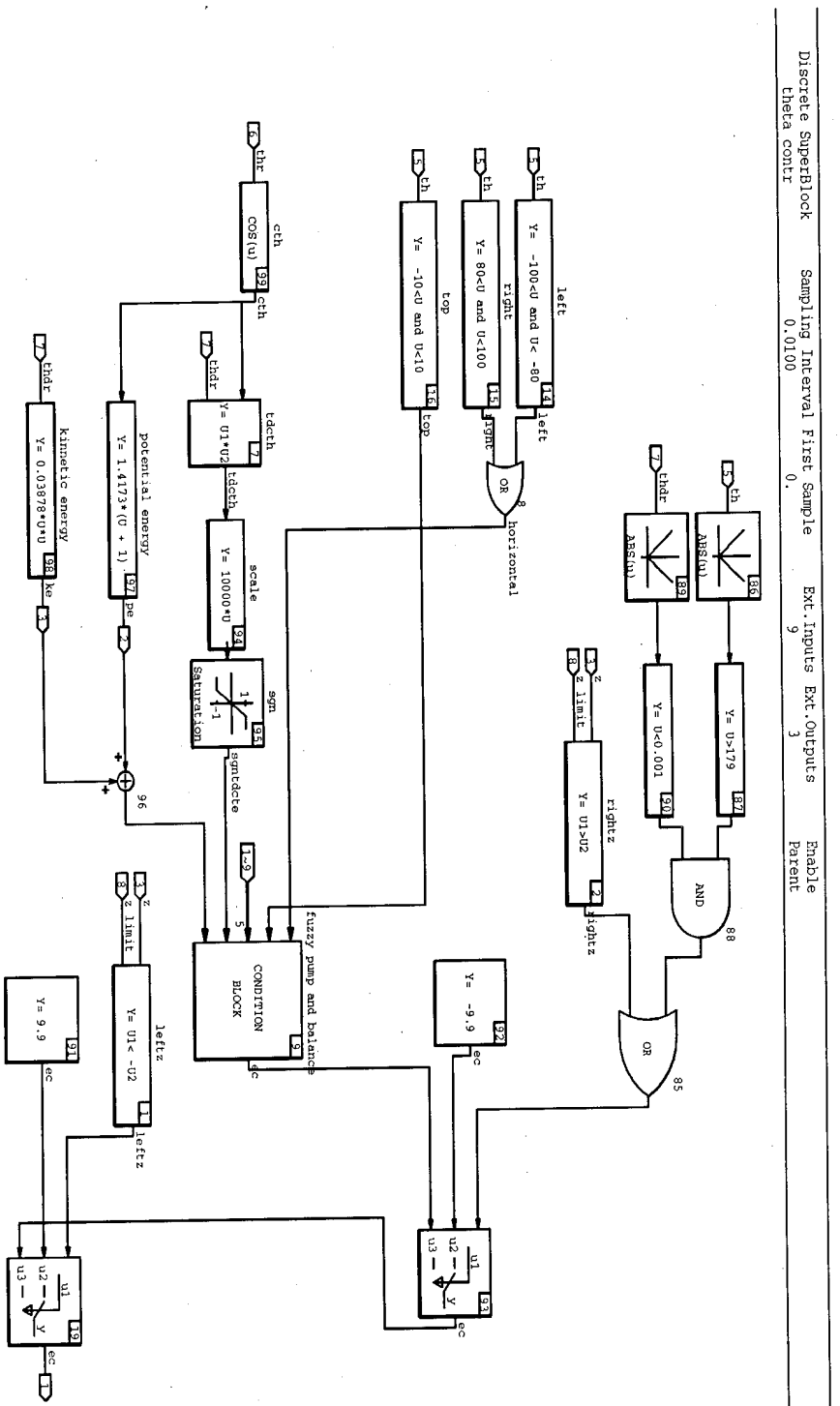

Figure D-9 Angle Controller

Figure D-10 Balancing Fuzzy Controller

Figure D-11 Energy Based Pump-Up Controller

Figure D-12 Adjust Z Position Controller

Appendix E

Membership Curves

E.1 Balancing Controller

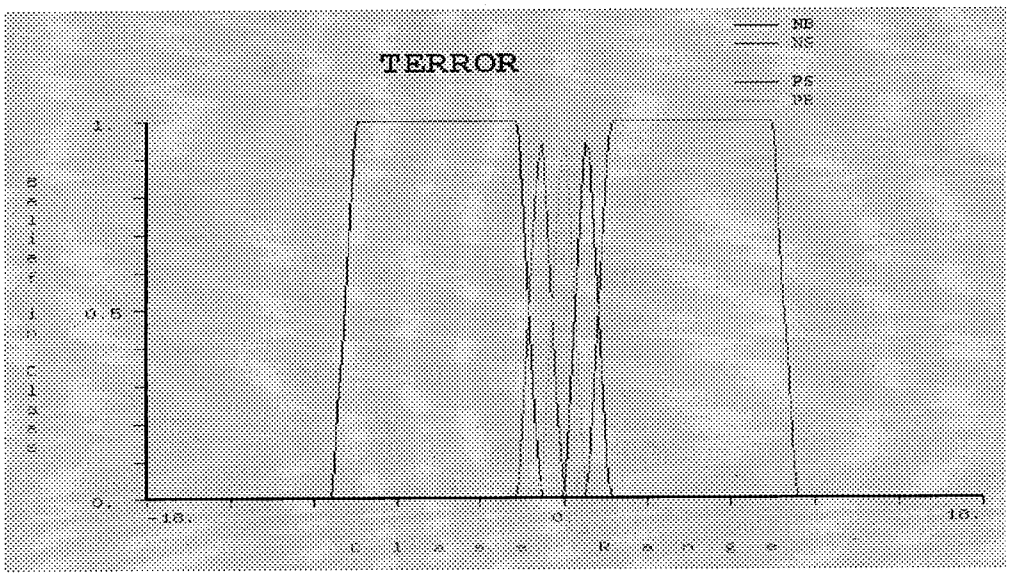

Figure E-1 Angular Error in Balancing Controller (input)

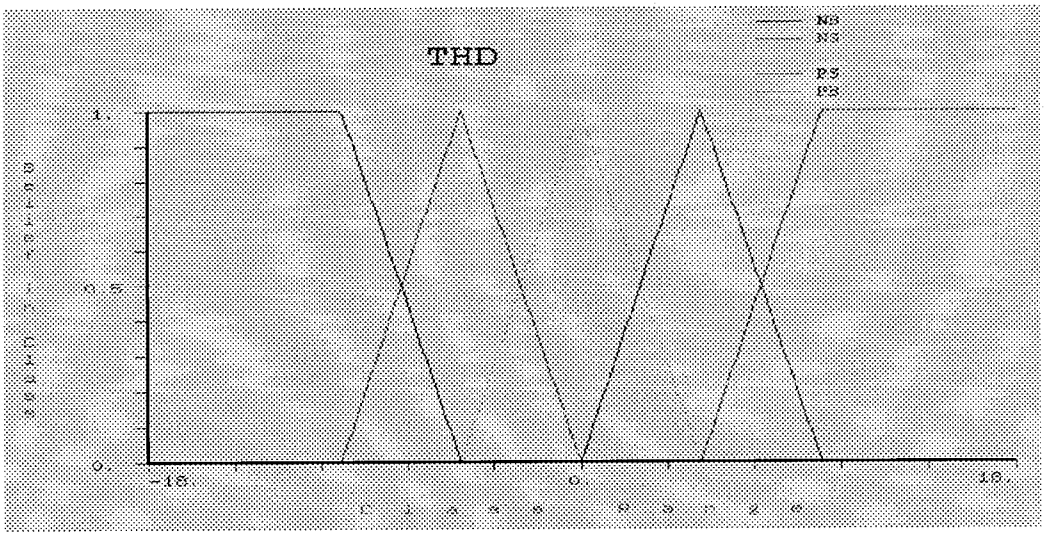

Figure E-2 Angular Rate in Balancing Controller (input)

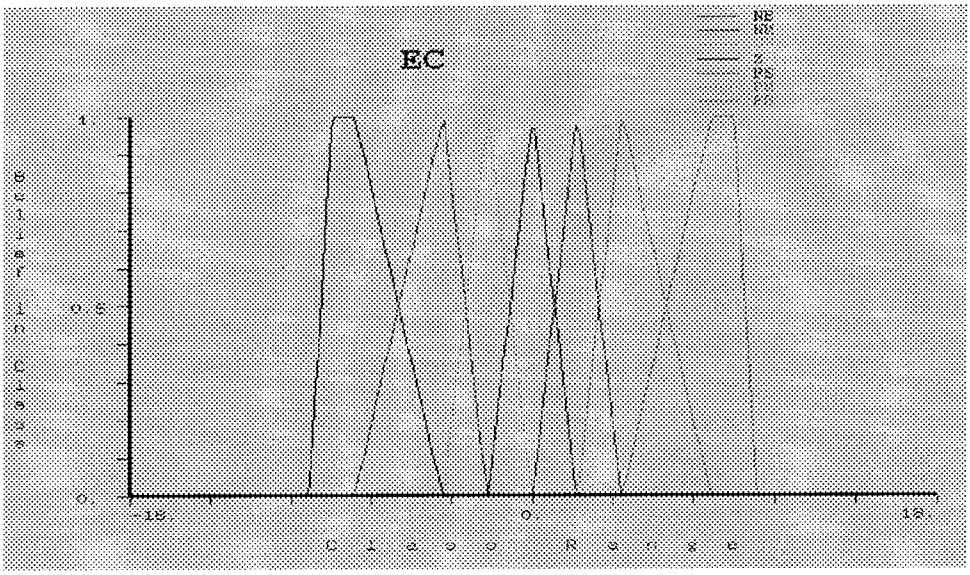

Figure E-3 Control Voltage in Balancing Controller (output)

E.2 Centering Controller

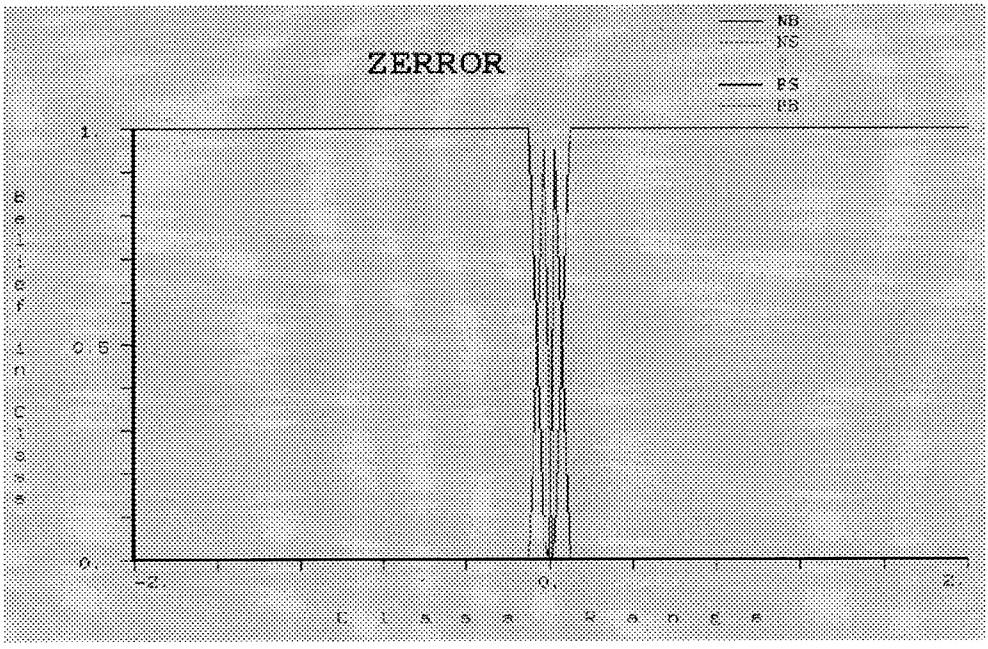

Figure E-4 Cart Position Error in Centering Controller (input)

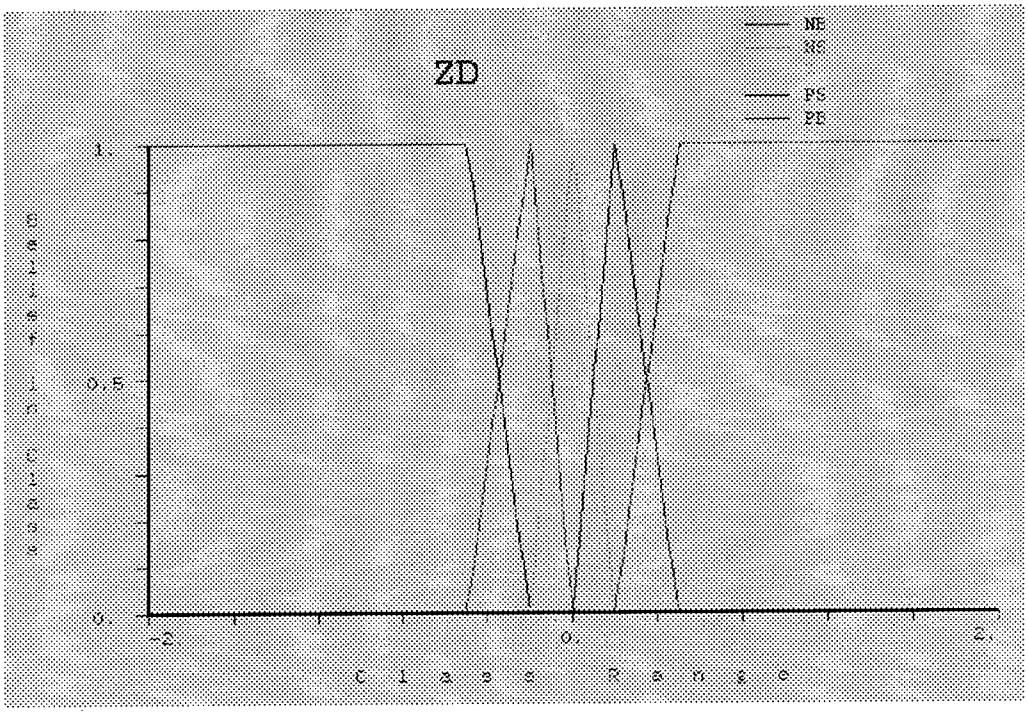

Figure E-5 Cart Velocity in Centering Controller (input)

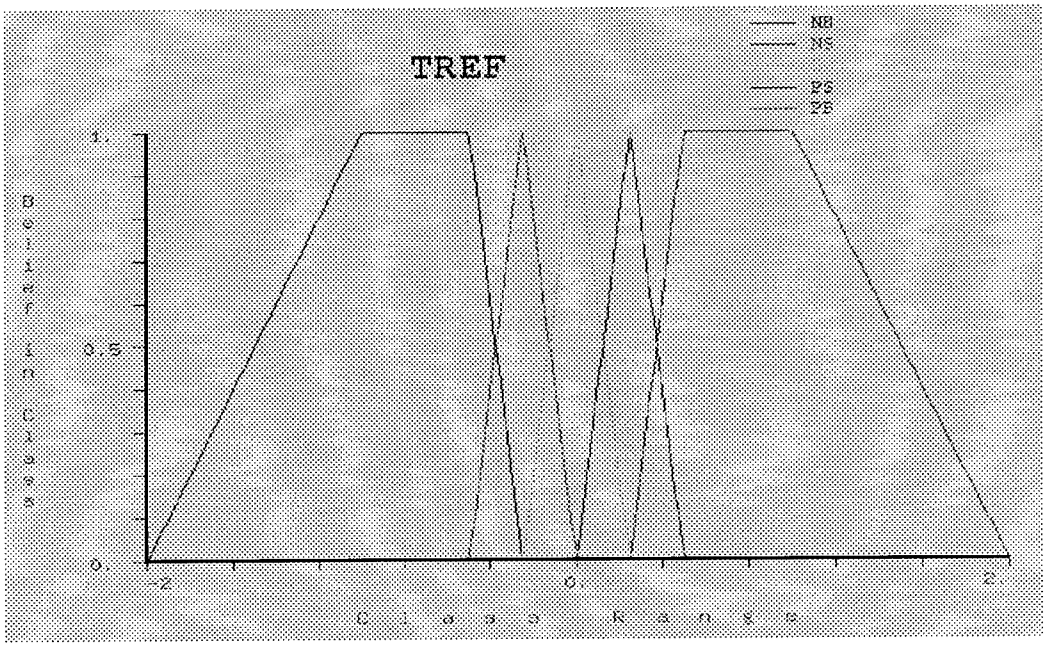

Figure E-6 Reference Angle in Centering Controller (output)

E.3 Friction Compensator

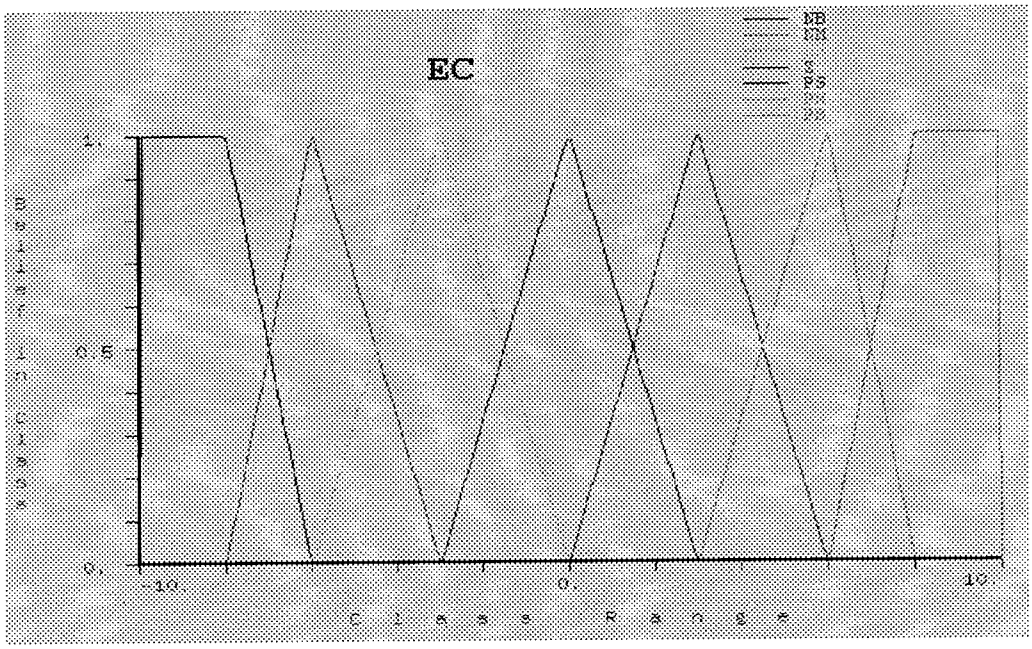

Figure E-7 Control Voltage in Friction Compensator (input)

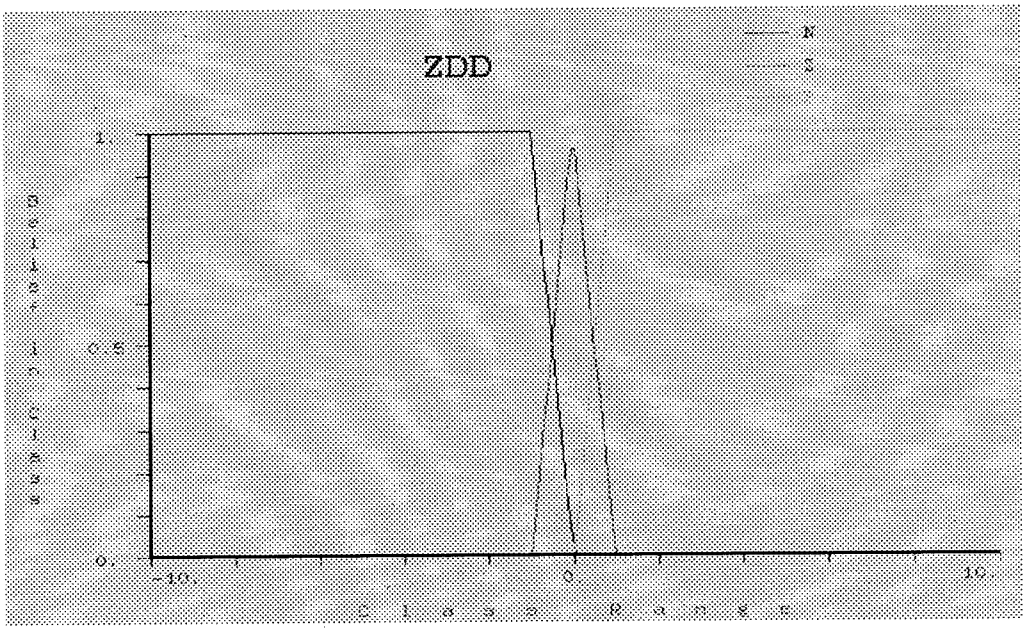

Figure E-8 Cart Acceleration in Friction Compensator (input)

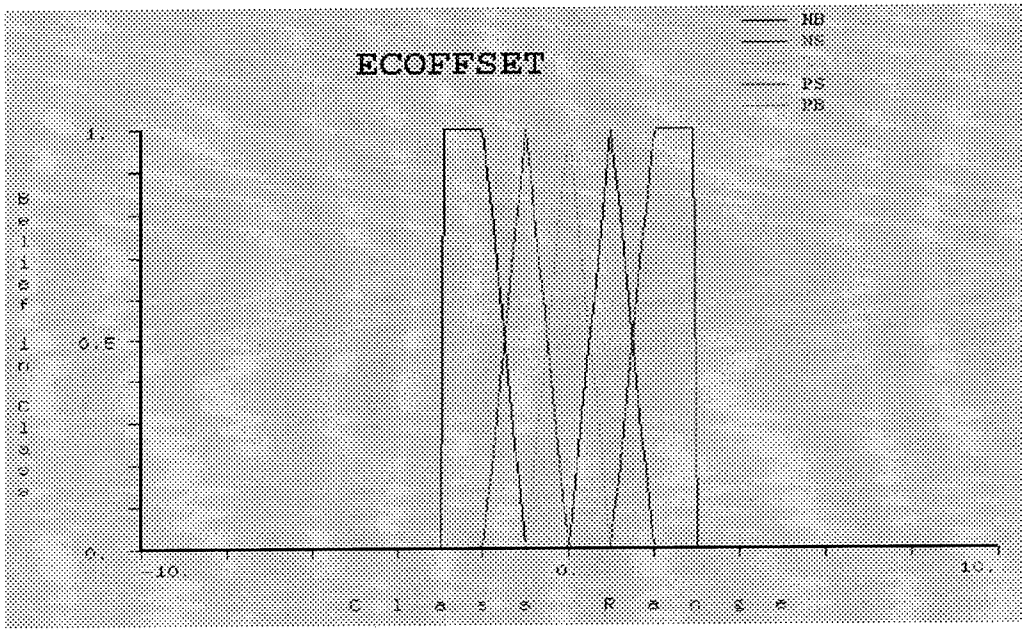

Figure E-9 Control Voltage Offset in Friction Compensator (output)

E.4 Pump Up Controller

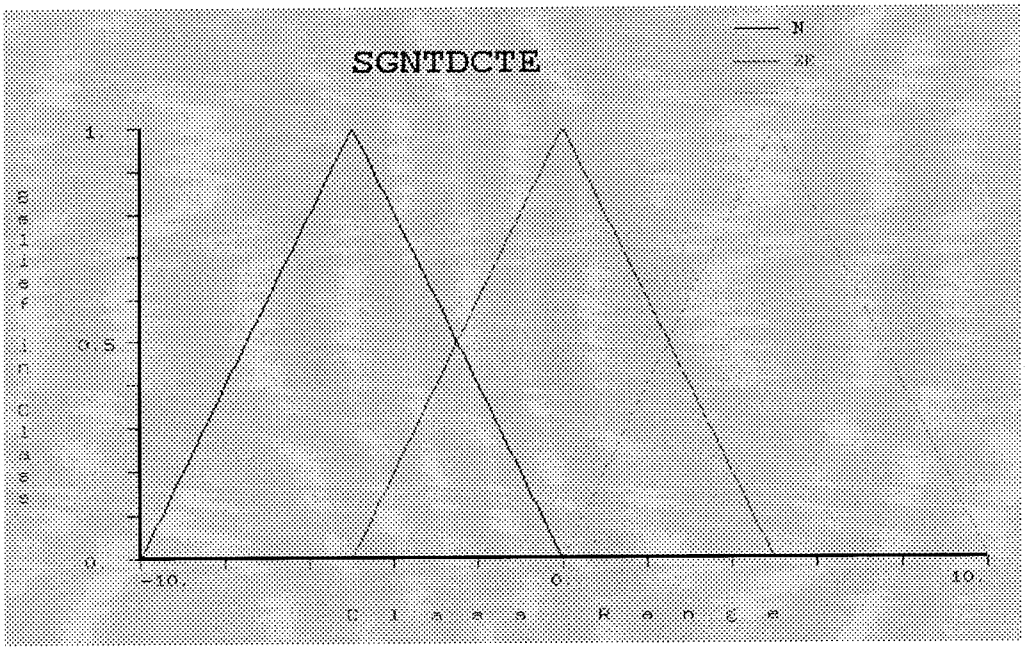

Figure E-10 $\theta_d \cos\theta$ in Pump Up Controller (input)

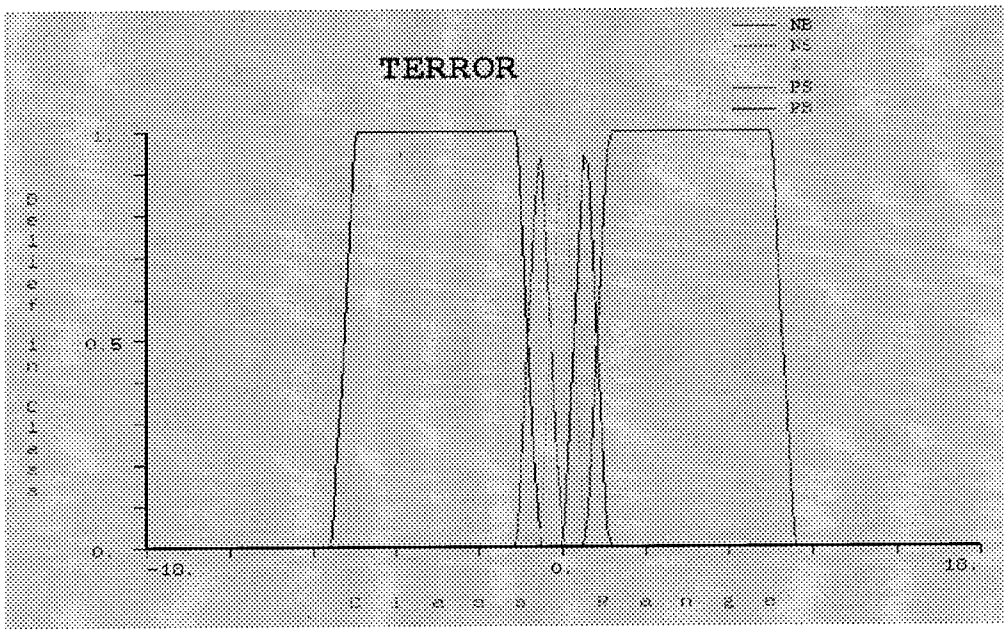

Figure E-11 Total Energy in Pump Up Controller (input)

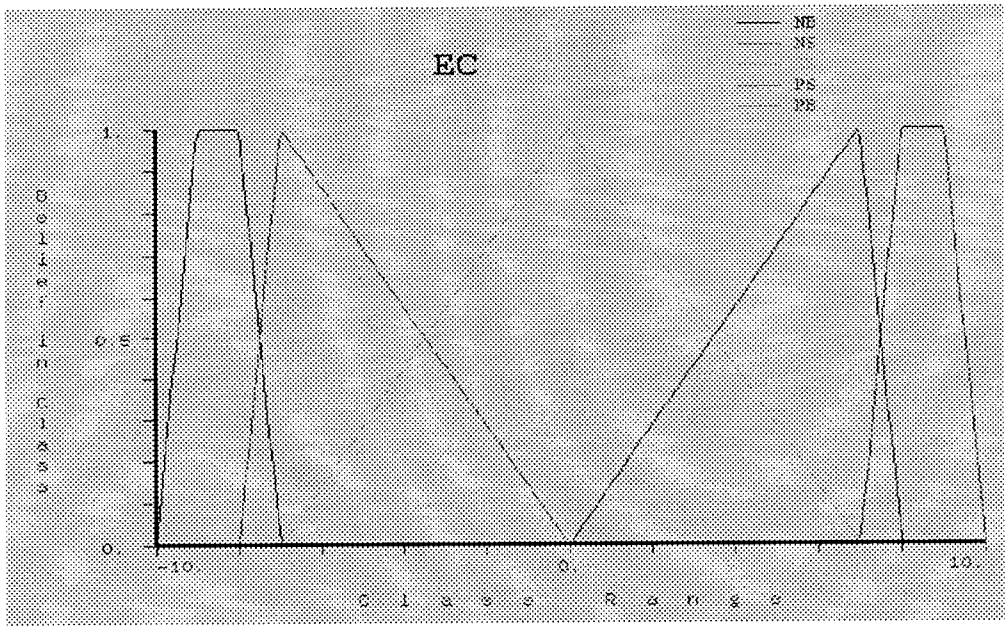

Figure E-12 Control Voltage in Pump Up Controller (output)

E.5 Controller for Z Adjustment in Pump Up

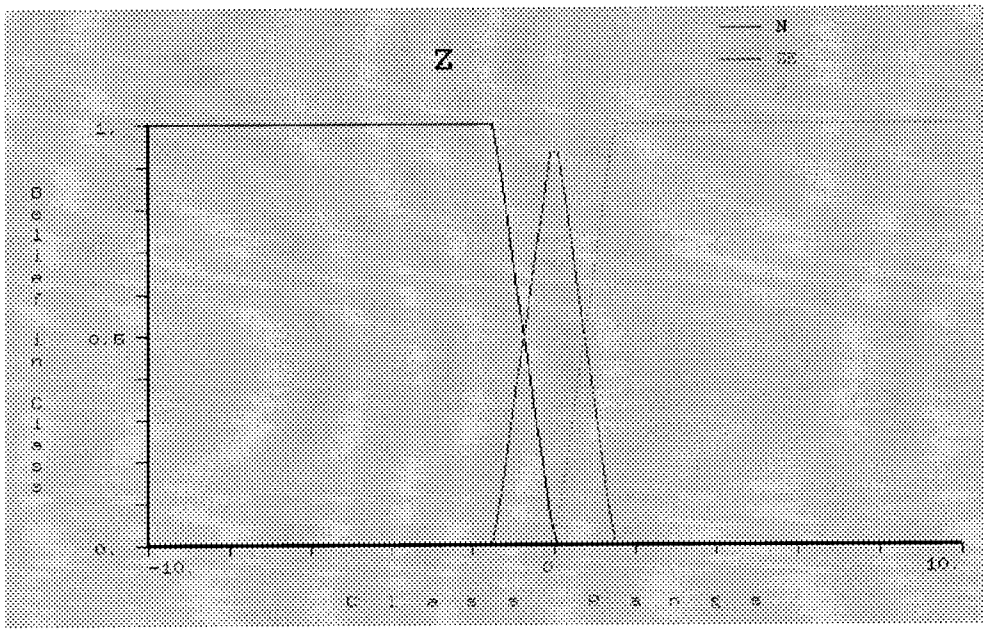

Figure E-13 Cart Position in Z Adjust Controller (input)

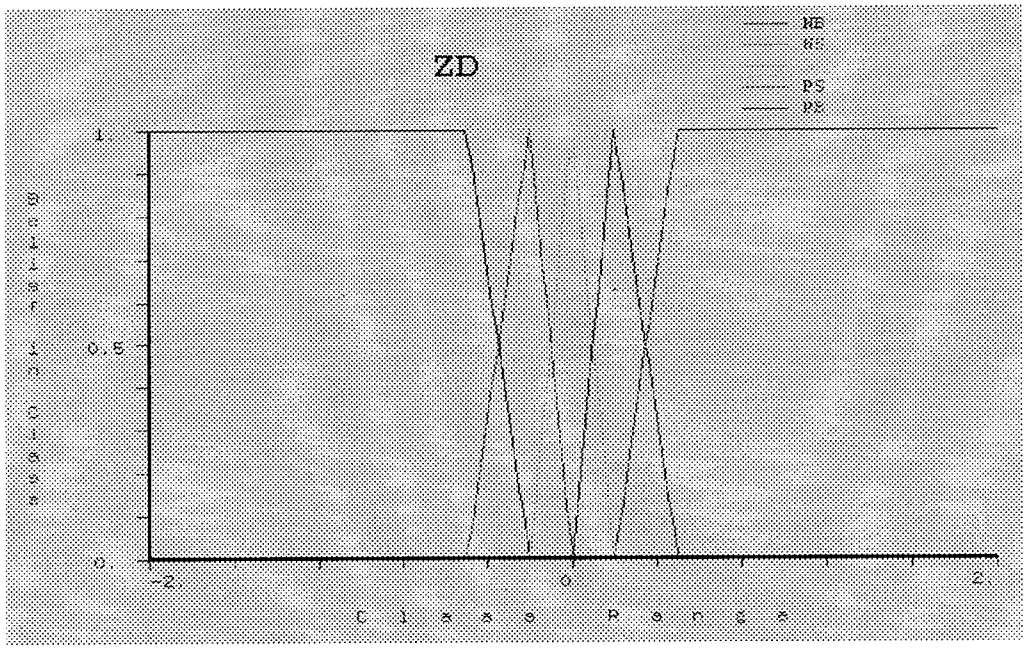

Figure E-14 Cart Velocity in Z Adjust Controller (input)

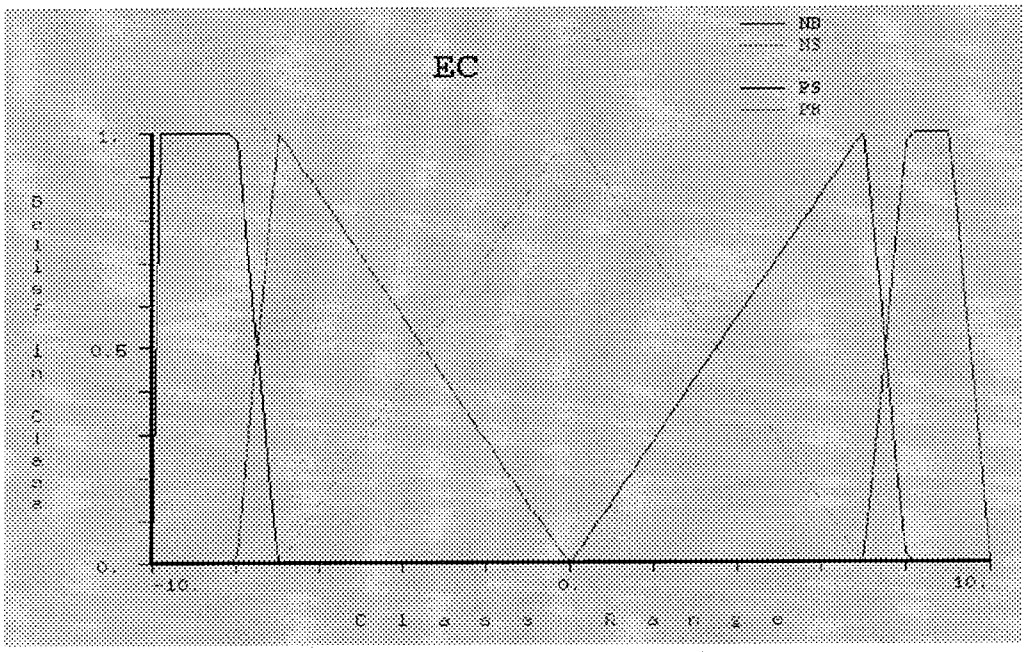

Figure E-15 Control Voltage in Z Adjust Controller (output)